Received: 1 October 2019 | Accepted: 15 February 2020

DOI: 10.1111/gcb.15069

PRIMARY RESEARCH ARTICLE

Global Change Biology WILEY

Reforestation and surface cooling in temperate zones: Mechanisms and implications

Quan Zhang[1,2] | Mallory Barnes[2] | Michael Benson[2] | Elizabeth Burakowski[3] | A. Christopher Oishi[4] | Andrew Ouimette[3] | Rebecca Sanders-DeMott[3] | Paul C. Stoy[5,6] | Matt Wenzel[7] | Lihua Xiong[1] | Koong Yi[8] | Kimberly A. Novick[2]

[1]State Key Laboratory of Water Resources and Hydropower Engineering Science, Wuhan University, Wuhan, China

[2]O'Neill School of Public and Environmental Affairs, Indiana University, Bloomington, IN, USA

[3]Institute for the Study of Earth, Oceans, and Space, University of New Hampshire, Durham, NH, USA

[4]Coweeta Hydrologic Laboratory, Southern Research Station, USDA Forest Service, Otto, NC, USA

[5]Department of Biological Systems Engineering, University of Wisconsin–Madison, Madison, WI, USA

[6]Department of Land Resources and Environmental Sciences, Montana State University, Bozeman, MT, USA

[7]National Ecological Observatory Network, Battelle, Jamestown, ND, USA

[8]Department of Environmental Sciences, University of Virginia, Charlottesville, VA, USA

Correspondence
Quan Zhang, State Key Laboratory of Water Resources and Hydropower Engineering Science, Wuhan University, Wuhan, China.
Email: quan.zhang@whu.edu.cn

Funding information
NSFC-NSF, Grant/Award Number: 51861125102; NASA-ROSES, Grant/Award Number: NNX17AE69G; NSF-DEB, Grant/Award Number: 1552747, 1637522, 1802726, 0823293 and 1440485; National Science Foundation, Grant/Award Number: 1552976, 1241881 and 1702029; National Institute of Food and Agriculture, Grant/Award Number: 228396, W3188 and 1006997; EPSCoR, Grant/Award Number: 1832959, 1920908 and 1101245; Forest Service; EPA, Grant/Award Number: 13-IA-11330140-044; Agriculture and Food Research, Grant/Award Number: 2012-67019-19484

Abstract

Land-use/cover change (LUCC) is an important driver of environmental change, occurring at the same time as, and often interacting with, global climate change. Reforestation and deforestation have been critical aspects of LUCC over the past two centuries and are widely studied for their potential to perturb the global carbon cycle. More recently, there has been keen interest in understanding the extent to which reforestation affects terrestrial energy cycling and thus surface temperature directly by altering surface physical properties (e.g., albedo and emissivity) and land–atmosphere energy exchange. The impacts of reforestation on land surface temperature and their mechanisms are relatively well understood in tropical and boreal climates, but the effects of reforestation on warming and/or cooling in temperate zones are less certain. This study is designed to elucidate the biophysical mechanisms that link land cover and surface temperature in temperate ecosystems. To achieve this goal, we used data from six paired eddy-covariance towers over co-located forests and grasslands in the temperate eastern United States, where radiation components, latent and sensible heat fluxes, and meteorological conditions were measured. The results show that, at the annual time scale, the surface of the forests is 1–2°C cooler than grasslands, indicating a substantial cooling effect of reforestation. The enhanced latent and sensible heat fluxes of forests have an average cooling effect of −2.5°C, which offsets the net warming effect (+1.5°C) of albedo warming (+2.3°C) and emissivity cooling effect (−0.8°C) associated with surface properties. Additional daytime cooling over forests is driven by local feedbacks to incoming radiation. We further show that the forest cooling effect is most pronounced when land surface

temperature is higher, often exceeding −5°C. Our results contribute important observational evidence that reforestation in the temperate zone offers opportunities for local climate mitigation and adaptation.

KEYWORDS
albedo, energy balance, reforestation, temperature, turbulent fluxes

1 | INTRODUCTION

Over the past two centuries, one of the most remarkable modes of global land-use/cover change (LUCC) has been the transition of forests to croplands (Goldewijk, 2001) and vice versa (Rudel et al., 2005). In some areas like the eastern United States, widespread deforestation has later been followed by substantial reforestation (Hooker & Compton, 2003; Manson & Evans, 2007; Mather, 1992; Ramankutty, Heller, & Rhemtulla, 2010; Wear & Greis, 2012). From the mid-19th to early 20th centuries, harvesting for timber and clearing for agriculture dramatically reduced forest cover by more than 90% in many areas of the eastern United States (Hall, Motzkin, Foster, Syfert, & Burk, 2002). By 1930, widespread land clearing had largely abated, and forest cover increased following the abandonment of marginal agricultural fields and active reforestation efforts (Wear & Greis, 2012). Thus, forest cover increased over the eastern United States for much of the 20th century.

Shifts between forests and short-statured ecosystems like grasslands and croplands have been widely studied for their potential to affect local-to-global carbon budgets (Houghton, Hackler, & Lawrence, 1999; Law et al., 2018). Anthropogenic and naturally caused deforestation is responsible for significant carbon dioxide (CO_2) emissions to the atmosphere (van der Werf et al., 2009; Woodwell et al., 1983). Conversely, reforestation has been proposed as a climate mitigation tool to enhance the size of the terrestrial carbon sink (Bastin et al., 2019; Law et al., 2018; Pan et al., 2011; Stoy et al., 2008) because of forests' potential to remove anthropogenic CO_2 (House, Prentice, & Le Quere, 2002). However, the persistence of current levels of forest carbon uptake into the future is uncertain, due to productivity limitations from increasing drought likelihood (Frank et al., 2015; Green et al., 2019), pest infestation (Boyd et al., 2019), and fire (Buotte et al., 2019).

More recently, attention has turned toward understanding the potential for changing forest cover to affect land surface temperature (T_s) directly by modifying ecosystem surface and biophysical properties, and thereby the energy balance (Anderson-Teixeira et al., 2012; Bright et al., 2017; Burakowski et al., 2018; Huang, Zhai, Liu, & Sun, 2018; Juang, Katul, Siqueira, Stoy, & Novick, 2007; Lee et al., 2011; Rigden & Li, 2017; Zhai, Liu, Liu, Zhao, & Huang, 2014). T_s is a state variable reflecting land surface–atmosphere feedbacks driven by water and energy exchange, and it is linked to surface aerodynamic and ecophysiological processes dependent on land cover (Bonan, 2008, 2016; Foley, Costa, Delire, Ramankutty, & Snyder, 2003; Pielke et al., 1998). For example, albedo, which is inversely related to T_s, changes as a function of multiple variables influenced by LUCC including snowpack depth, leaf area index, surface color, and canopy structure. In particular, darker, denser forests with a lower albedo absorb more solar radiation, which in isolation has a warming effect when compared to nearby grasslands (Juang et al., 2007; Lee et al., 2011). Non-radiative forcings linked to biophysical processes, like sensible heat flux and latent heat flux (i.e., energy dissipated in the form of evapotranspiration), are also key determinants of the surface energy budget and also impact T_s (Liu, Liu, & Baig, 2019). The greater sensible and latent heat fluxes, which are closely related to aerodynamic and ecophysiological properties of the land cover, cool the surface (Luyssaert et al., 2014). For example, in semi-arid environments, forests reduce aerodynamic resistance and increase sensible heat flux (Banerjee, De Roo, & Mauder, 2017; Eder, Schmidt, Damian, Traumner, & Mauder, 2015), thereby having the potential to cool the surface though the corresponding transpiration is usually low. The roles of turbulent fluxes remain less understood because they are subject to varying hydrologic conditions and surface–atmosphere feedbacks like changes in atmospheric boundary layer height (Baldocchi et al., 2001; Baldocchi & Ma, 2013; Novick & Katul, 2020; Vick, Stoy, Tang, & Gerken, 2016). Nonetheless, in tropical zones, it is relatively well understood that forests are cooler than non-forested ecosystems as a result of the higher forest evaporative cooling effect (Bonan, 2008; Costa, 2005). In contrast, in boreal zones, forests are believed to be warmer than non-forested ecosystems due to the predominant warming effect of lower forest albedo, whereas short-statured ecosystems are often covered by snow with higher albedo (Bonan, 2008; Lee et al., 2011; Swann, Fung, Levis, Bonan, & Doney, 2010).

In temperate zones, however, results are mixed, and it is unclear precisely how LUCC impacts T_s (Lejeune, Davin, Gudmundsson, Winckler, & Seneviratne, 2018). Much of the relevant work in the temperate zone has been done at regional to global scales based on remote sensing data (e.g., Bright et al., 2017; Peng et al., 2014; Schultz, Lawrence, & Lee, 2017; Wickham, Wade, & Riitters, 2013), where it is possible to draw inference about broad patterns in temperature, but it is challenging to link those dynamics to mechanistic forcings (Lee et al., 2011). Some studies show that deforestation over temperate zones cools the local environment by driving coupled climate and land surface models under contrasting land use scenarios (Feddema et al., 2005; Hansen et al., 1998), while others reported the opposite (Alkama & Cescatti, 2016; Jackson et al., 2005; Ramankutty, Delire, & Snyder, 2006). In the eastern temperate United States, a coupled land–atmosphere model and tower observations were used to demonstrate that forest warming in winter is driven primarily by albedo, while summer cooling is more strongly influenced by surface canopy roughness (Burakowski et al., 2018). By using

empirical models driven by flux tower observations, Bright et al. (2017) predict that non-radiative forcings dominate the temperature response to LUCC, and reforestation has an overall cooling effect in the temperature zone. By using MODIS T_s products (MYD11A2), Wickham et al. (2013) suggest that forests in temperate zones tend to cool the surface, though the responsible mechanisms were not identified. Schultz et al. (2017) identified diurnal asymmetry, with forests warming the surface at night and cooling during the day relative to open lands in temperate zones, attributed to differences in albedo, latent heat flux, and surface roughness. In summary, these regional-scale studies, informed largely by models or remote sensing data, highlight the potential for local cooling by reforestation in the temperate zone, but leave the mechanisms as to how reforestation impacts T_s largely unclear.

More mechanistic understanding is possible at the site level, enabled by flux tower records that permit quasi-continuous observation of the exchange of water, energy, and carbon between the atmosphere and the land surface at ecosystem scales (Baldocchi et al., 2001). A few studies have used flux tower data to quantify the relative contributions of different factors to the LUCC-induced T_s change. For example, Juang et al. (2007) successfully separated the effects of surface albedo and ecophysiological properties on T_s in a grassland, pine forest, and deciduous forest co-located in the North Carolina Piedmont, though the analysis was limited to well-watered conditions. Lee et al. (2011) blended flux tower observations and meteorological station data from northern latitudes to deduce that deforestation in boreal zones has a cooling effect, due largely to the resulting increase in albedo, but the same conclusion could not be made for the temperate zone. More recently, Burakowski et al. (2018) highlighted the important cooling effect of enhanced surface roughness in forests growing in North Carolina and New Hampshire. These prior studies advance our understanding of biophysical mechanisms determining LUCC-induced T_s change, but we still lack a general and mechanistic accounting of the overall balance between evaporative and aerodynamic cooling versus albedo-driven warming in temperate zones.

Even less is known about how hydro-climatic conditions influence relationships between LUCC and T_s, as this has not been a focus of previous site-level work (e.g., Burakowski et al., 2018; Juang et al., 2007; Lee et al., 2011). Drought is predicted to become more frequent and severe in the future (Cook, Ault, & Smerdon, 2015), driven substantially by large increases in atmospheric vapor pressure deficit (VPD; Ficklin & Novick, 2017; Zhang et al., 2019). Evidence is accumulating that changing soil and atmospheric moisture deficits are driving long-term patterns in water fluxes (Jackson et al., 2005; Jung et al., 2010; Novick et al., 2016; Rigden & Salvucci, 2017). Trees and grasses have contrasting plant water use strategies (Konings, Williams, & Gentine, 2017) and regulate water uptake differently during hydrologic stress, thereby affecting the amount of energy dissipated as latent heat (Bonan, 2008; Teuling et al., 2010). The impact of drought on T_s is therefore important to resolve when evaluating the climate mitigation potential of reforestation.

To address these knowledge gaps, we compared T_s and its mechanistic drivers from six paired forest and grassland flux towers that span a wide range of latitudes in the temperate eastern United States. We adopt a framework that decomposes T_s difference between forests and grasslands into its individual contributing factors (Luyssaert et al., 2014) to study the impacts of different mechanisms and varying hydrologic stress conditions. The major goals are to (a) quantify temporal variation of T_s differences between forests and grasslands (ΔT_s) in temperate zones, (b) explain the mechanisms and quantify the effects of aerodynamic and ecophysiological properties on ΔT_s, and (c) investigate the role that hydro-climatic conditions play in contributing to ΔT_s. We hypothesize that the temperate forests are cooler than nearby grasslands due to enhanced turbulence transfer of sensible and latent heat fluxes. We further hypothesize that forests will sustain greater latent heat flux during drought when compared to grasslands, such that the forests will be even more cooler than grasslands during periods of hydrologic stress. The results of this study will expand our understanding of the usefulness of reforestation as a climate mitigation strategy to directly affect local temperature, now and in the future when more extreme climate conditions are expected.

2 | MATERIALS AND METHODS

2.1 | Site description and paired flux towers

Our study uses data from six paired forest–grassland towers spanning a wide range of latitudes in the temperate eastern United States (see Figure 1 and Table 1). The forests include deciduous, needleleaf evergreen, and mixed stands. The grasslands are all predominantly

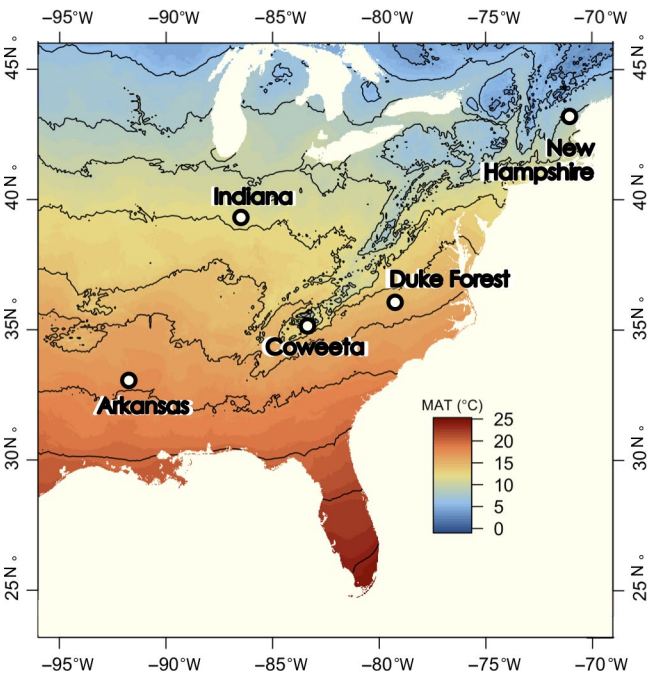

FIGURE 1 The location of our study sites with the mean annual temperature (MAT) as the background. All locations support one grassland–forest tower pair, except Duke Forest, where a grassland tower is co-located with a hardwood and a pine forest stand. There are altogether 11 individual flux towers in this study [Colour figure can be viewed at wileyonlinelibrary.com]

C3 ecosystems managed with seasonal harvest, or as pastureland. Similar to other studies using a paired-site approach to investigate ecosystem energy cycling (Lee et al., 2011; Luyssaert et al., 2014), the forest and grassland towers of each pair in our study are 0.7–27.4 km apart (see Table 1) to ensure that macro-scale climate conditions do not vary appreciably (Barry, 1970). The northernmost pair is located in New Hampshire where towers were installed over a mixed evergreen needleleaf and deciduous broadleaf temperate forest (referred to as NH-Mixed hereafter) and a co-located grassland (referred to as NH-Grass hereafter; Burakowski et al., 2018). In south-central Indiana, we use data from two AmeriFlux sites—the 20-year-old Morgan Monroe State Forest site (IN-Broadleaf hereafter) and the Bayles Road grassland site (IN-Grass hereafter), which was installed in 2016. We incorporate two tower clusters located in North Carolina and Georgia. From western North Carolina, a deciduous broadleaf-forested AmeriFlux site situated within the Coweeta Hydrologic lab (CW-Broadleaf hereafter) is paired with a grassland site established in a nearby cow pasture in 2016 (referred to as CW-Grass hereafter) just across the state line in Georgia. In central North Carolina, we included the three Duke Forest AmeriFlux sites, where the Duke Forest-Hardwood site (DK-Broadleaf hereafter) and the Duke Forest-Loblolly Pine site (DK-Needleleaf hereafter) are paired with the Duke Forest-Open Field grassland site (DK-Grass hereafter). Finally, the southernmost site cluster is located in Arkansas, where the Crossett Experimental Forest AmeriFlux site (AR-Needleleaf hereafter) is paired with a newly established grassland site in the Overflow National Wildlife Refuge (AR-Grass hereafter), also installed in 2016. Thus, there are 11 individual sites in this study (see Table 1 for details). An analysis of long-term meteorological information available from the DAYMET dataset (https://daymet.ornl.gov/) revealed that the annual precipitation and temperature of the site-specific study periods were close to the long-term means (results not shown); or in other words, the study periods did not include extreme climate events. Among all the sites, only the New Hampshire site is consistently covered by snow in winter. For the 2012–2018 period, there were 34 days with snow >15.24 cm, 47 days with snow >10.16 cm, 55 days with snow >7.62 cm, and 71 days with snow >0 cm on average. Snow is intermittent at other sites. Much of our analysis is particularly focused on the growing season, defined as May–August, when leaf area is relatively stationary.

2.2 | Measurements of the radiation components and environmental variables

On each tower, the incoming and outgoing short- and long-wave radiation (R_{si}, R_{so}, R_{li}, and R_{lo}, respectively) were measured using a four-component radiometer (CRN1 or CRN4, Kipp & Zonen, Delft, Netherlands). The surface albedo (i.e., α) was inferred as the ratio of mid-day outgoing and incoming short-wave radiation ($\alpha = R_{so}/R_{si}$), and the radiometric surface temperature can be inferred from R_{lo} using the Stefan–Boltzmann law as described below. Air temperature (T_a), relative humidity (RH), and precipitation (P) were measured at all towers. See Table 1 for the heights of all measurements. The instrumentation for NH-Mixed, NH-Grass, IN-Broadleaf, CW-Broadleaf, DK-Broadleaf, DK-Needleleaf, and DK-Grass towers is described in detail in the references given in Table 1. At the IN-Grass, CW-Grass, AR-Needleleaf, and AR-Grass towers, T_a and RH were monitored with HMP-type probes (Vaisala, Helsinki, Finland), and P with a tipping bucket (TE525, Texas Electronics). Soil heat flux (G) was monitored at IN, CW, and AR clusters using HFP-01 soil heat flux plates (Hukseflux Thermal Sensors).

2.3 | Eddy covariance measurement, flux processing, and quality control

On each tower, an eddy covariance (EC) system was used to measure the net ecosystem exchange of CO_2, latent heat flux (LE), sensible heat flux (H), wind speed (u), and friction velocity (u^*). Each EC system consisted of an infrared gas analyzer and a three-dimensional sonic anemometer, though instruments differ from site to site. At NH-Mixed and NH-Grass, an enclosed-path analyzer (LI-7200, LI-COR) was paired with a WindMaster sonic anemometer (Gill Instruments Limited). At IN-Broadleaf, a closed-path analyzer (LI-7000, LI-COR) was paired with a CSAT3 sonic anemometer (Campbell Scientific). At IN-Grass, a combined open-path analyzer and sonic system was deployed (IRGASON, Campbell Scientific). At CW-Broadleaf and AR-Needleleaf, an enclosed-path analyzer (EC-155, Campbell Scientific) was paired with an RM Young 8100 sonic anemometer (RM Young Company). At CW-Grass, DK-Broadleaf, DK-Needleleaf, DK-Grass, and AR-Grass, an open path gas analyzer LI-7500 (LI-COR) was paired with a CSAT3 (Campbell Scientific) sonic anemometer. While instrument-related biases are a concern when comparing non-identical EC systems (Novick et al., 2018), measures were taken to reduce uncertainty linked to experimental design. These include the application of an analytical spectral correction to fluxes measured with closed- and enclosed-path sensors (see Sulman, Roman, Scanlon, Wang, & Novick, 2016 for details of IN-Broadleaf; Novick et al., 2013 for details of CW-Broadleaf and AR-Needleleaf; Fratini, Ibrom, Arriga, Burba, & Papale, 2012 for the methods used for NH-Mixed and NH-Grass) and routine calibration of the analyzers (approximately weekly to monthly for the closed- and enclosed-path systems, and seasonally for the open path systems). A side-by-side comparison of an LI-7500 and EC155 system revealed biases in the fluxes to be relatively low at CW-Broadleaf provided that data collected with a high wind speed angle of attack were removed (Novick et al., 2013). The IN-Broadleaf, CW-Broadleaf, and AR-Needleleaf towers have all benefitted from a direct evaluation of flux integrity by hosting the AmeriFlux roving Portable Eddy Covariance System (Ocheltree & Loescher, 2007), with favorable results.

As all data shared to the AmeriFlux network, raw high-frequency data from our study sites were converted into half-hourly or hourly fluxes using site-specific algorithms. These are described for the Duke Forest sites in Novick et al. (2015), for the

TABLE 1 Location, data range, and climate characteristics of the 11 eddy covariance towers used in the present study

Site ID	AmeriFlux site ID	Site name	State	Location	Data coverage	Separation distance (km)
NH-Mixed	—	Thompson Farm	New Hampshire	43°07′N, 70°57′W	6/1/2016–5/31/2017	5.7
NH-Grass	—	Kingman Farm	New Hampshire	43°10′N, 70°56′W		
IN-Broadleaf	US-MMS	Morgan Monroe State Forest	Indiana	39°19′N, 86°25′W	7/1/2017–6/30/2018	15
IN-Grass	US-BRG	Bayles Road Grassland	Indiana	39°13′N, 86°32′W		
CW-Broadleaf	US-Cwt	Coweeta Hydrologic Laboratory	North Carolina	35°04′N, 83°26′W	8/1/2017–7/31/2018	11.5
CW-Grass	-	Rabun Gap Grassland	Georgia	34°58′N, 83°24′W		
DK-Broadleaf	US-Dk2	Duke Forest-hardwoods	North Carolina	35°58′N, 79°08′W	1/1/2005–12/31/2008	0.8
DK-Needleleaf	US-Dk3	Duke Forest-loblolly pine	North Carolina	35°58′N, 79°08′W		0.7
DK-Grass	US-Dk1	Duke Forest-open field	North Carolina	35°58′N, 79°08′W		
AR-Needleleaf	US-Cst	Crossett Experimental Forest	Arkansas	33°03′N, 91°55′W	6/1/2016–5/31/2017	27.4
AR-Grass	—	Crossett Overflow Grassland	Arkansas	33°07′N, 91°38′W		

CW-Broadleaf in Oishi et al. (2018), for the NH-Mixed and NH-Grass towers in Burakowski et al. (2018), and for IN-Broadleaf in Sulman, Roman, Scanlon, et al. (2016). The processing procedures for AR-Needleleaf are identical to those for CW-Broadleaf. For the three newly established IN-Grass, CW-Grass, and AR-Grass towers, fluxes were processed using an algorithm similar to that developed for open-path systems described in Novick et al. (2013), in which a 2D coordinate rotation was applied, raw data were despiked using the algorithm of Papale et al. (2006), and the Webb–Pearman–Leuning correction for density effects was applied (Webb, Pearman, & Leuning, 1980).

Finally, we applied a standard post-processing and gap-filling approach to all the data using the REddyProc online tool (https://www.bgc-jena.mpg.de/REddyProc/brew/REddyProc.rhtml, Wutzler et al., 2018). The online tool filters out data collected during stable atmospheric conditions using u^* filtering, and gap-fills missing data using a marginal distribution sampling approach. Finally, all measurements were aggregated to the hourly time scale for the comparative analysis.

2.4 | Decomposing the surface temperature difference between forests and grasslands

In this study, the T_s difference between forests and grasslands is defined as:

$$\Delta T_s = T_{s,\text{forest}} - T_{s,\text{grassland}}, \quad (1)$$

such that ΔT_s is negative when forests are cooler than grasslands.

To understand how different components of the energy budget affect ΔT_s, we adopt a framework that decomposes ΔT_s into its multiple contributing components after Luyssaert et al. (2014) as described below. The net radiation (R_n) can be written as the sum of the incoming and outgoing short- and long-wave radiation:

$$R_n = R_{si} - R_{so} + R_{li} - R_{lo}. \quad (2)$$

Here, R_{so} can be expressed as a function of R_{si} and α as $R_{so} = \alpha R_{si}$ such that Equation (2) can be rearranged to:

$$R_n = (1-\alpha) R_{si} + R_{li} - R_{lo}. \quad (3)$$

R_n can also be expressed in terms of the ecosystem energy fluxes:

$$R_n = LE + H + G + I, \quad (4)$$

where I is a residual imbalance that is necessary when using EC measurements in practice, which often do not achieve full energy balance closure (Foken, 2008). At sites where soil heat fluxes were unavailable, G was set to zero.

By combining Equations (3) and (4), we eliminate R_n:

$$(1-\alpha) R_{si} + R_{li} - R_{lo} = LE + H + G + I. \quad (5)$$

The R_{lo} can be expressed as a function of the surface temperature (i.e., T_s) using the Stefan–Boltzmann law:

Elevation a.s.l. (m)	MAT (°C)	MAP (mm)	Canopy height (m)	Measurement height (m)	Ecosystem type	Reference	Data source (DOI)
40	8.9	1,170	35	30	Mixed evergreen needleleaf–deciduous broadleaf forest	Burakowski et al. (2018)	–
33	8.9	1,170	0.2–1	3.6	Grassland	Burakowski et al. (2018)	–
275	10.8	1,094	34	46	Deciduous broadleaf forest	Schmid et al. (2000)	https://doi.org/10.17190/AMF/1246080
180	10.8	1,094	0.2–0.5	3	Grassland	This study	–
690	12.9	1,495	30	37	Deciduous broadleaf forest	Oishi et al. (2018)	–
657	12.9	1,495	0.2–0.5	3	Grassland	This study	–
168	14.36	1,170	25	39	Deciduous broadleaf forest	Novick et al. (2015)	https://doi.org/10.17190/AMF/1246047
163	14.36	1,170	18	21	Evergreen needleleaf forest	Novick et al. (2015)	https://doi.org/10.17190/AMF/1246048
168	14.36	1,170	0.55	2.7	Grassland	Novick et al. (2004)	https://doi.org/10.17190/AMF/1246046
50	17.4	1,410	27	37	Evergreen needleleaf forest	This study	–
31	17.4	1,410	0.2–1.0	3	Grassland	This study	–

$$R_{lo} = A\sigma\varepsilon T_{s,obs}^4, \quad (6)$$

where A is the view factor assumed to be equal to 1, σ is the Stefan–Boltzmann constant, and ε is the surface emissivity. Following the treatment by Juang et al. (2007), ε is approximated by an empirical relationship with the albedo as $\varepsilon = -0.16\alpha + 0.99$.

Combining Equations (5) and (6) gives:

$$(1-\alpha)\,R_{si} + R_{li} - \sigma\varepsilon T_s^4 = LE + H + G + I. \quad (7)$$

From Equation (7), the full derivative of ΔT_s can be estimated using a first-order Taylor series approximation as (Luyssaert et al., 2014):

$$\Delta T_s = \frac{1}{4\sigma\varepsilon T_s^3}\left[-R_{si}\delta\alpha + (1-\alpha)\,\delta R_{si} + \delta R_{li} - \delta LE - \delta H - \delta G - \delta I - \sigma T_s^4 \delta\varepsilon\right]. \quad (8)$$

Note that $\delta(\bullet)$ denotes the difference of each variable between the forest and grassland, for example, $\delta\alpha = \alpha_{forest} - \alpha_{grassland}$. Here, for simplicity, the contributions of within-site differences in R_{si} and R_{li} are combined into a single term, the incoming radiation, that is, $\delta R_i = (1-\alpha)\,\delta R_{si} + \delta R_{li}$ so that Equation (8) becomes:

$$\Delta T_{s,cal} = \frac{1}{4\sigma\varepsilon T_s^3}\left[-R_{si}\delta\alpha + \delta R_i - \delta LE - \delta H - \delta G - \delta I - \sigma T_s^4 \delta\varepsilon\right], \quad (9)$$

where $\Delta T_{s,cal}$ is the calculated temperature change across space (e.g., from one tower to the next) reflecting contributions from different components of the energy balance. Hereafter, we use $\delta T_s(\bullet)$ to represent the value of each contributing component to ΔT_s, including albedo ($\delta T_s(\alpha)$), incoming radiation ($\delta T_s(R_i)$), latent heat flux ($\delta T_s(LE)$), sensible heat flux ($\delta T_s(H)$), ground heat flux ($\delta T_s(G)$), the residual of EC energy balance ($\delta T_s(I)$), and emissivity ($\delta T_s(\varepsilon)$). Noting that the subscript "cal" in Equation (9) denotes the calculated surface temperature difference derived by summing the difference attributable to the individually measured components. In contrast, the subscript "obs" refers to the surface temperature difference inferred directly from the outgoing long-wave radiation by solving Equation (6) for temeprature.

This analysis was conducted at the hourly time scale after filtering the data by the following criteria: (a) data were filtered to exclude rain events (P > 0 mm); (b) the hourly $\Delta T_{s,obs}$ (by solving Equation 6) was compared with $\Delta T_{s,cal}$ (Equation 9), and we only accepted records when $\Delta T_{s,obs}$ and $\Delta T_{s,cal}$ have the same sign and the difference is less than a threshold of 2°C. As illustrated in Figure S1, the choice of this threshold has little effect on the root mean square error (RMSE) of the observed and calculated annual ΔT_s, over the range of 1.5–4°C. We selected 2°C to achieve the minimal RMSE while retaining a large percentage of the data. The $\Delta T_{s,cal}$ was very close to the $\Delta T_{s,obs}$ when considering data for the entire year, as well as records collected within and outside of the growing season and non-growing season, at multiple time scales (see Figures S2 and S3). This agreement between observed and estimated surface temperature difference validates the use of Equation (9) to understand the mechanistic basis of the $\Delta T_{s,obs}$. When calculating the albedo, only daytime records from 9:00 to

15:00 local time were used to derive the daily average, which was then used throughout the corresponding day.

2.5 | The role of aerodynamic and ecophysiological properties in determining the ΔT_s between forests and grasslands

The surface-to-air temperature difference and the bulk aerodynamic conductance (g_a) are the two key determinants of the sensible heat flux (H):

$$H = \rho C_p g_a \left(T_s - T_a\right), \tag{10}$$

where ρ is the air density and C_p (=1,004.67 J kg^{-1} K^{-1}) is the specific heat of air at constant pressure. The g_a can be determined from the wind speed (u) and friction velocity (u^*; Monteith & Unsworth, 1990) as follows:

$$g_a = \left(\frac{u}{u*^2} + 6.2u*^{-\frac{2}{3}}\right)^{-1}. \tag{11}$$

Friction velocity depends on features of canopy height and structure and tends to be higher over rougher surfaces like forests (Kelliher, Leuning, & Schulze, 1993). Thus, LUCC impacts on H are largely linked to impacts on g_a. This approach also explicitly incorporates g_a into the attribution of ΔT_s as recommended by Rigden and Li (2017).

To explore how ecophysiological properties impact the T_s difference, we investigated the dynamics of surface conductance (G_s), which can be determined from the measured LE fluxes by inverting the Penman–Monteith equation (Monteith, 1965):

$$G_s = \frac{\gamma LE g_a}{\Delta\left(R_n - G\right) + \rho C_p \mathrm{VPD} g_a - LE\left(\Delta + \gamma\right)}, \tag{12}$$

where Δ is the slope of saturated water vapor pressure curve against air temperature, γ is the psychrometric constant determined as $P_A C_p / 0.622\lambda$, where P_A is the air pressure and λ is the latent heat of vaporization. For decades, surface conductance estimated in this way has been viewed as a proxy for bulk canopy stomatal conductance, to link stomatal function, evapotranspiration, and the drivers of each (Kim & Verma, 1991; Li et al., 2019; Novick et al., 2016; Stoy et al., 2006; Sulman, Roman, Yi, et al., 2016; Wever, Flanagan, & Carlson, 2002; Wilson & Baldocchi, 2000; Zhang et al., 2019). Although G_s is not a perfect proxy for stomatal conductance, as it contains information reflecting both stomatal and soil resistance to evaporation, these difficulties can be minimized through careful data screening – for example, by removing data when the canopy is wet (Li et al., 2019; Sulman, Roman, Yi, et al., 2016; Zhang et al., 2019). In dense canopies like those studied here, where little radiation is available to drive soil evaporation, G_s tends to be dominated by canopy stomatal conductance, particularly when the canopy is dry (Stoy et al., 2006; Zhang et al., 2019).

2.6 | Linking ΔT_s to variations in hydro-climate during the growing season

As a final step in our analysis, we explored how ΔT_s varied as a function of VPD, which integrates information about temperature and hydrologic conditions. While soil moisture (Porporato, Laio, Ridolfi, & Rodriguez-Iturbe, 2001; van Beek, Wada, & Bierkens, 2011) and VPD (Lemordant, Gentine, Swann, Cook, & Scheff, 2018; Novick et al., 2016; Zhang et al., 2019) are both commonly used indicators of hydrologic stress, in mesic ecosystems of the eastern United States, VPD has been shown to be the dominant driver affecting plant function during periods of hydrologic stress (Novick et al., 2016). Moreover, although soil moisture and VPD tend to be decoupled at short time scales (hours to days), they are strongly correlated at time scales of weeks and longer (Novick et al., 2016; Zhou et al., 2019), and tower-based observations of VPD are more readily available and integrate over larger land areas when compared to the soil moisture, which is usually measured at only a few locations in the flux tower footprint (if at all). We focused this analysis specifically on the response of latent and sensible heat fluxes to VPD, and complimented the analysis with an exploration of how the response of canopy surface conductance to VPD varies within the paired sites. Surface conductance was estimated by inverting the observed latent heat flux records using the Penman–Monteith equation (Equation 12, also see Zhang et al., 2019). To reduce the confounding effect of radiation, we constrained the analysis to periods when $R_{si} \geq 400$ W/m^2, noting that results were relatively insensitive to the choice of the radiation threshold provided it was above 350 W/m^2. To reduce uncertainty linked to phenological variation, we constrained this analysis to the growing season. The hourly ΔT_s between forests and grasslands was then binned by VPD, using increments of 0.2 kPa.

3 | RESULTS

3.1 | Forests are generally cooler than co-located grasslands

The surface of the forests was generally cooler (negative values) than the grasslands at most sites. The probability density functions of the hourly $\Delta T_{s,obs}$ between forests and grasslands reveal that annual mean $\Delta T_{s,obs}$ was −1.3°C for NH, −0.0°C for IN, −1.4°C for CW, −1.6°C for DK-Needleleaf, −0.8°C for DK-Broadleaf, and −0.4°C for AR (Figure 2). At most sites, the median of $\Delta T_{s,obs}$ was very close to the mean, except for IN where the mean of $\Delta T_{s,obs}$ (−0.0°C) was substantially higher than the median (−0.8°C).

3.2 | The diurnal and seasonal variations in ΔT_s

The mean diurnal ΔT_s exhibited a unimodal pattern with a peak around noontime (Figure 3). Forests were cooler than grasslands during

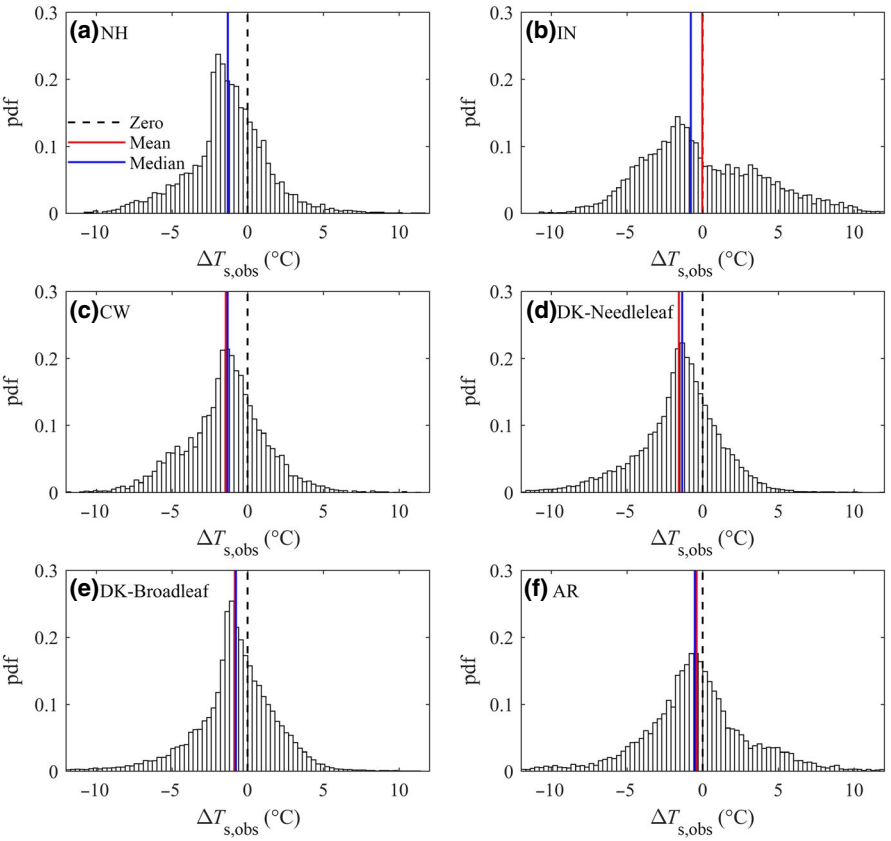

FIGURE 2 The probability density function (pdf) of the observed hourly surface temperature difference ($\Delta T_{s,obs}$) between forests and grasslands for the six paired sites (a–f). Dashed vertical lines represent $\Delta T_{s,obs}$ of 0°C, and red and blue vertical lines represent the mean and median, respectively. AR, Arkansas; CW, Coweeta; DK-Broadleaf, Duke Forest-Hardwood; DK-Needleleaf, Duke Forest-Loblolly Pine; IN, Indiana; NH, New Hampshire [Colour figure can be viewed at wileyonlinelibrary.com]

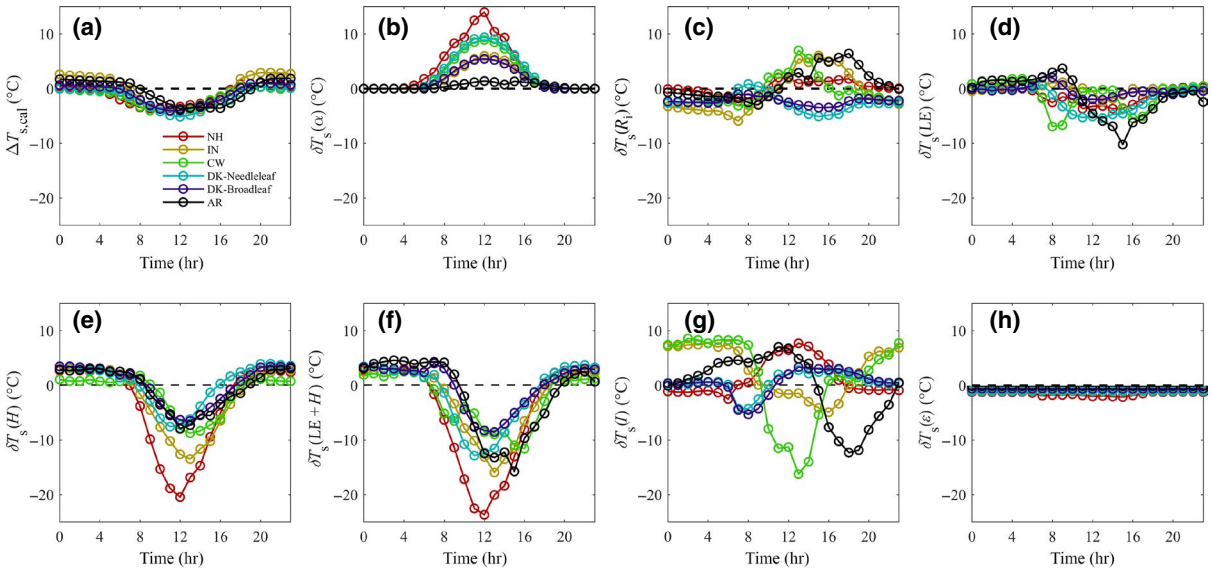

FIGURE 3 The mean diurnal variation of the calculated radiometric surface temperature ($\Delta T_{s,cal}$) between forests and grasslands (a) and the calculated contributions from the terms of Equation (9) (b–h); negative ΔT_s implies that forests and cooler than grasslands per our convention. Note that the variation associated with the ground heat flux was excluded due to insufficient measurements; the joint contribution of latent and sensible heat flux was provided in panel (f). Note that the calculated ΔT_s (i.e., $\Delta T_{s,cal}$ of panel a) by Equation (9) rather than the observed ΔT_s is compared with its decomposed components [Colour figure can be viewed at wileyonlinelibrary.com]

most of the daytime and were slightly warmer than grasslands during most of the nighttime across sites (Figure 3a). Among all the individual contributing factors, the albedo (Figure 3b) and sensible heat flux (Figure 3d) contributions had clear mid-day peaks, while the rest showed more diverse patterns. At all sites, incoming radiation tended to be greater in forests than grasslands in early morning hours, perhaps reflecting the influence of fog over the shorter grassland towers. During the mid-day hours, the patterns of differences in incoming radiation were less consistent and varied from one site to the next, which could reflect site-level instrumental bias. For most of the

contributing factors, the mean diurnal trend observed during both the growing season (Figure S4) and other parts of the year (Figure S5) were similar to the annual diurnal patterns. The daytime latent heat flux of forests outside of the growing season was substantially lower than grasslands at NH, IN, CW, and DK-Broadleaf, leading to a warming effect (Figure S5d).

Seasonal variations of the monthly averaged $\Delta T_{s,obs}$ showed diverse patterns across the six paired sites (Figure 4). At NH, CW, and

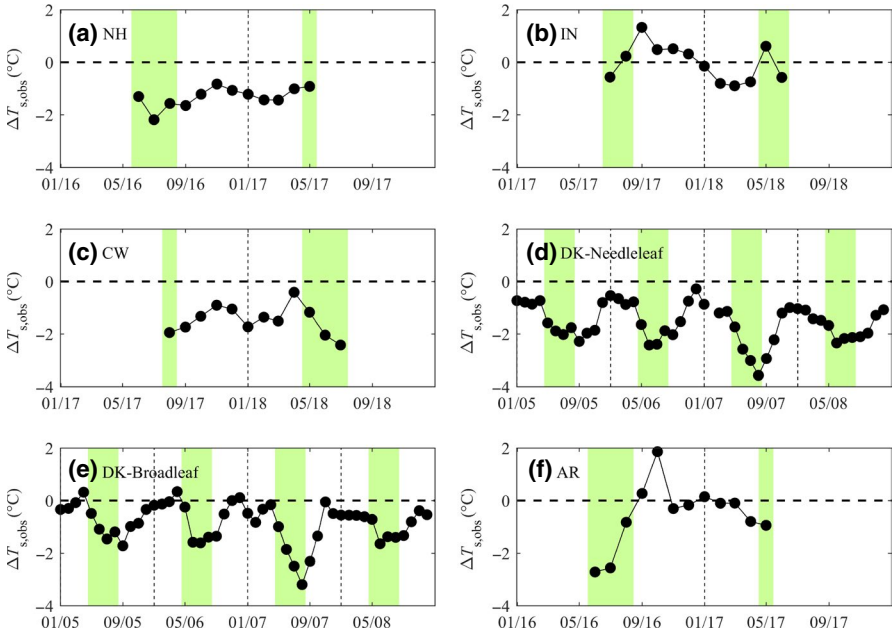

FIGURE 4 Seasonal variations of the observed monthly averaged temperature difference ($\Delta T_{s,obs}$) between forests and grasslands for the six paired sites (a–f). Hereafter, the vertical dashed line represents the month of January of the corresponding year, and the shaded green area represents the growing season (May, June, July, and August); the *x*-axis of date is formatted by mm/yy. AR, Arkansas; CW, Coweeta; DK-Broadleaf, Duke Forest-Hardwood; DK-Needleleaf, Duke Forest-Loblolly Pine; IN, Indiana; NH, New Hampshire [Colour figure can be viewed at wileyonlinelibrary.com]

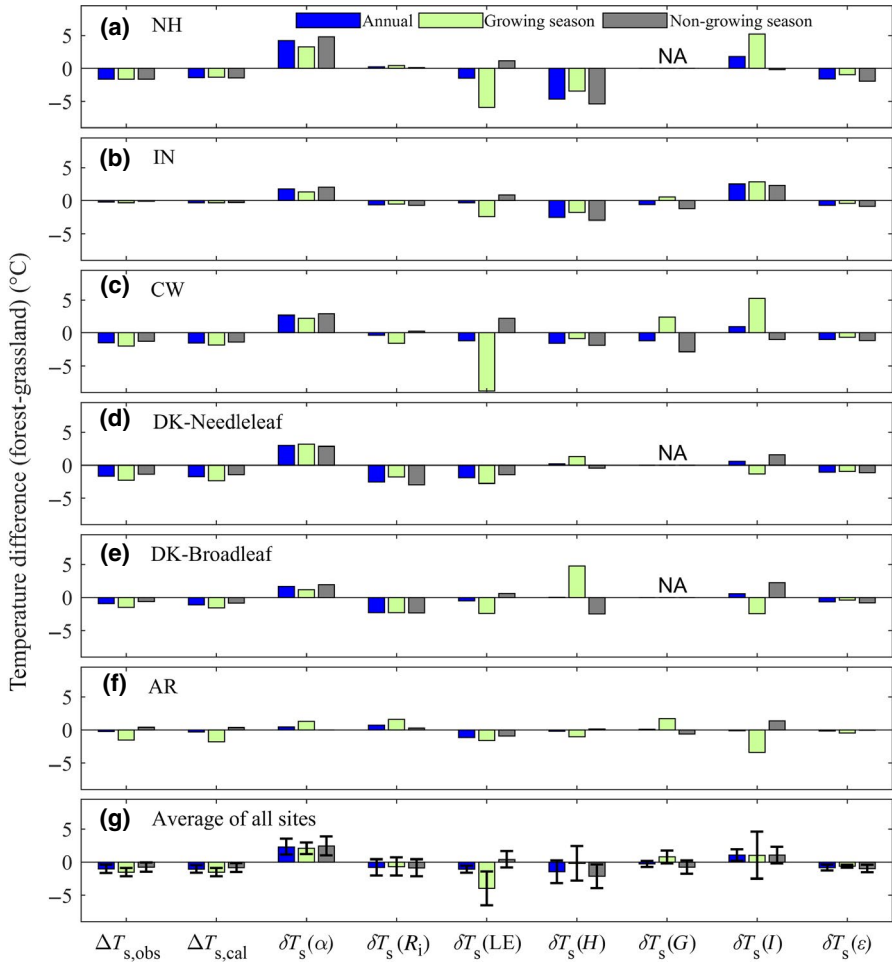

FIGURE 5 The observed and calculated annual (blue bar), growing season (green bar), and outside of the growing season (grey bar) forest–grassland temperature difference ($\Delta T_{s,obs}$ and $\Delta T_{s,cal}$) together with its contributing components described by Equation (9) for all the six paired sites (a–f) and the average across all the sites (g). Note that the error bar for panel (g) denotes the standard deviation of the six (three for *G*) site-averaged values. NA indicates sites without *G* records. AR, Arkansas; CW, Coweeta; DK-Broadleaf, Duke Forest-Hardwood; DK-Needleleaf, Duke Forest-Loblolly Pine; IN, Indiana; NH, New Hampshire [Colour figure can be viewed at wileyonlinelibrary.com]

DK-Needleleaf, the forests were consistently cooler than grasslands across the entire year (Figure 4a,c,d, respectively). At DK-Broadleaf and AR, forests were mostly cooler than grasslands during the growing season, but not during the rest of the year (Figure 4e,f). At IN, no clear seasonal pattern in $\Delta T_{s,obs}$ was observed (Figure 4b).

3.3 | The annual contribution of each component to ΔT_s between forests and grasslands

The overall cooling effect over forests of the six paired sites averaged about −1°C (annual $\Delta T_{s,obs}$ of −1.0 ± 0.6°C and $\Delta T_{s,cal}$ of −1.1 ± 0.6°C, Figure 5g) despite albedo differences between forests and grasslands that, if they operated in isolation, would consistently make all study forests warmer by +2.3°C on average (Figure 5g). Higher emissivity in forests counteracted the albedo-driven warming by −0.8°C on average. At most sites, higher *LE* and *H* of forests had a substantial cooling effect of −2.5°C on average, further offsetting the albedo-driven warming. The contributions of albedo and emissivity differed somewhat across seasons, but these seasonal patterns were less stark when compared to the seasonal trends for the contributions from *LE* and *H*. Contributions of the differences in R_i were observed at all sites (Figure 5a–f) and tended to cool the forests by −0.8°C. Where it was measured (IN, CW, and AR), soil heat flux (i.e., *G*) had a warming contribution to ΔT_s during the growing season, and cooling contribution otherwise. The overall contribution of *G* for the entire year was minor (−0.3°C on average) for all the three paired sites with *G* measured.

3.4 | The role of the aerodynamic and ecophysiological properties in determining ΔT_s between forests and grasslands

The surface–air temperature difference ($T_s - T_a$) was lower in forests than grasslands at almost all sites (Figure 6, first column). Furthermore, the surface–air temperature difference over both forests and grasslands had a clear seasonal pattern; specifically, it was steeper over both forests and grasslands during the growing season at most sites. The

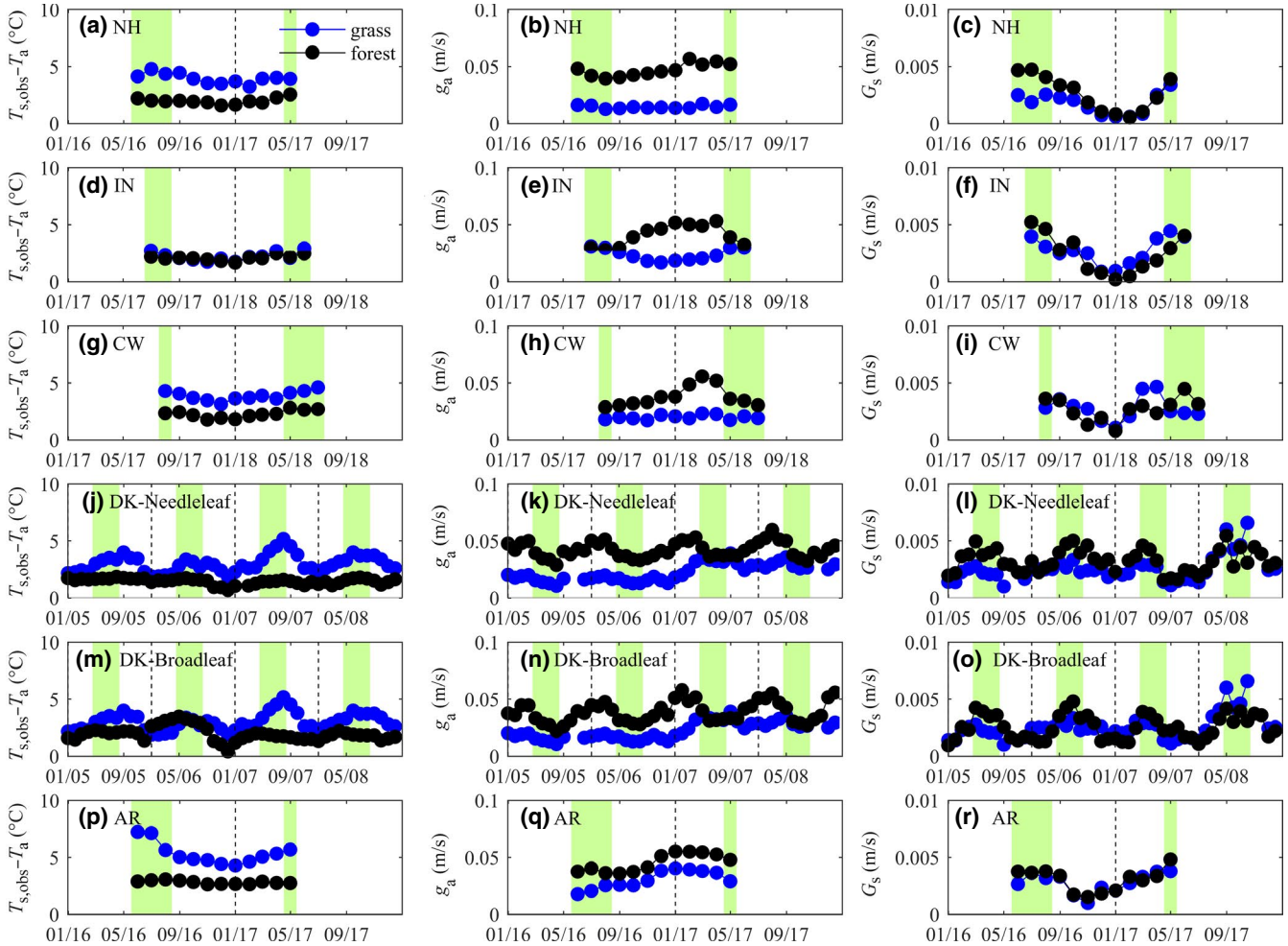

FIGURE 6 Seasonal variations of the monthly averaged surface–air temperature difference ($T_{s,obs} - T_a$, the first column), the aerodynamic conductance (g_a, the middle column), and the surface conductance (G_s, the right column) for both forests and grasslands across the six sites. Note that each row contains one site-pair. AR, Arkansas; CW, Coweeta; DK-Broadleaf, Duke Forest-Hardwood; DK-Needleleaf, Duke Forest-Loblolly Pine; IN, Indiana; NH, New Hampshire [Colour figure can be viewed at wileyonlinelibrary.com]

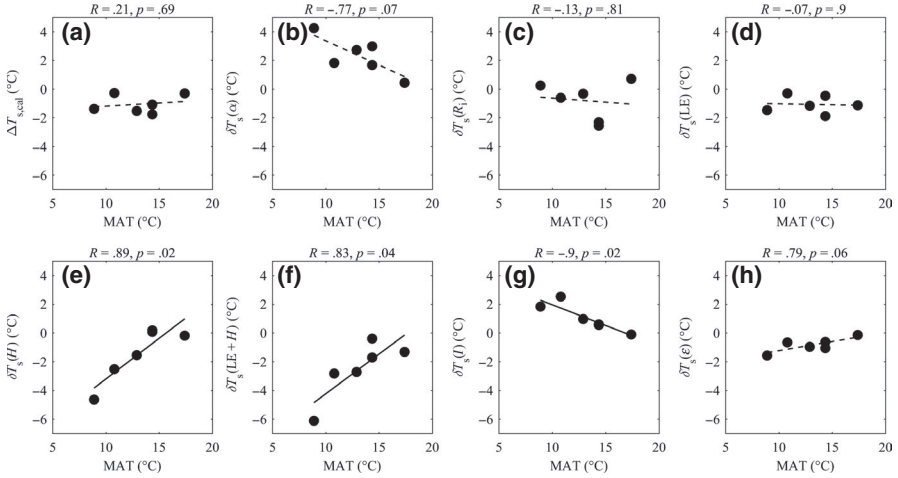

FIGURE 7 The correlation of the mean annual temperature (MAT) with the calculated annual temperature difference between forests and grasslands ($\Delta T_{s,cal}$) (a), as well as its components (b–h). Note that the result for ground heat flux was not presented due to the lack of measurements, instead, we provided the joint contribution of *LE* and H in panel (f); the coefficient of correlation (*R*) and significance of fitting (*p*) with *F*-test are provided at the top of each panel, and the linear fitting was shown in solid line for $p < .05$ and in dashed line for $p \geq .05$

lower surface–air temperature difference over forests was consistent with its higher g_a compared with grasslands (Figure 6, middle column). These large differences in g_a thereby drive substantially higher *H* over forests than grasslands at many sites. Differences in G_s between forests and grasslands across site pairs are less pronounced (Figure 6, right column). At NH, DK-Needleleaf, and DK-Broadleaf, the G_s of forests was substantially higher than grasslands during the growing season. Elsewhere, G_s was relatively similar much of the time, though it tended to be slightly higher in forests during the growing season.

3.5 | The components of ΔT_s vary with site mean annual temperature

Using the mean annual temperature (MAT) as a surrogate, the ΔT_s exhibited no clear dependence on the microclimate of each site (Figure 7a), but the relative importance of many ΔT_s components was influenced by site microclimate (Figure 7b–h). We found the role of albedo and emissivity was more pronounced at sites with lower MAT (Figure 7b,h). Though neither relationship was statistically significant at the level of $p < .05$, they may reflect the influence of snow, noting that winter snow cover is common at the NH sites and intermittent at the IN sites. Of the two ecophysiological mechanisms (*H* and *LE*), we examined for determining ΔT_s, *H* was strongly related to MAT and was most important in the coldest sites (Figure 7e), but *LE* did not show any significant trend with MAT (Figure 7d). When combining both turbulent fluxes of latent and sensible heat, we found the joint cooling effect of the *LE* and *H* to the ΔT_s was more pronounced at sites with lower MAT (Figure 7f), primarily driven by *H*.

3.6 | Linking ΔT_s to hydro-climatic conditions within the growing season

In most sites (DK-Needleleaf, DK-Broadleaf, NH, and AR), the cooling effect over forests was more pronounced when VPD was high (Figure 8a,d–f). In the IN site, no significant relationship between $\Delta T_{s,obs}$ and VPD was found (Figure 8b). In the CW site, a slight increase in $\Delta T_{s,obs}$ with rising VPD was observed (Figure 8c). In most sites, G_s declined with the rising VPD for both forests and grasslands (Figure S6), implying stomatal closure under high VPD. However, the difference in *LE* between forests and grasslands increased as a function of VPD in only three sites (NH, DK-Broadleaf, and AR, Figure 9a,e,f). In other sites, patterns were less clear, and

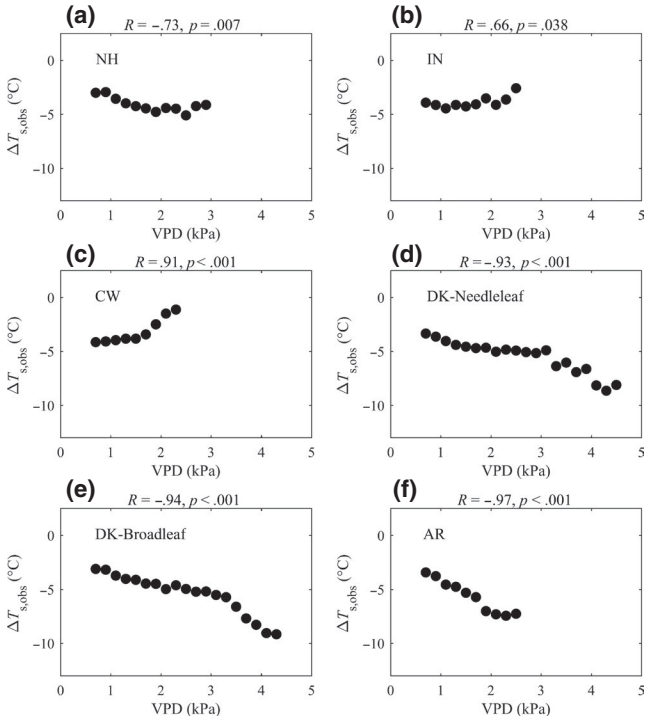

FIGURE 8 The correlation of the observed temperature difference ($\Delta T_{s,obs}$) between forests and grasslands with the vapor pressure deficit (VPD) when incoming short-wave radiation (R_{si}) is non-limiting (i.e., $R_{si} \geq 400$ W/m^2) during the growing season (May, June, July, and August) for all the six paired sites (a–f). Note that the samples are binned by VPD for every 0.2 kPa, and the bar denotes the standard error of all available records within the bin. The coefficient of correlation (*R*) and significance of fitting (*p*) with *F*-tests are provided at the top of each panel. AR, Arkansas; CW, Coweeta; DK-Broadleaf, Duke Forest-Hardwood; DK-Needleleaf, Duke Forest-Loblolly Pine; IN, Indiana; NH, New Hampshire

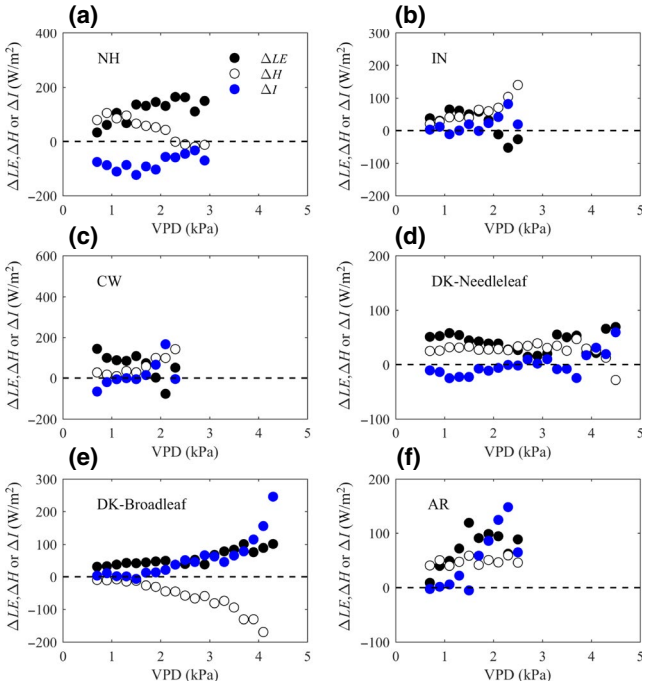

FIGURE 9 The observed latent heat flux difference (Δ*LE*), sensible heat flux difference (Δ*H*), and the residual of energy balance (Δ*I*) between forests and grasslands under different vapor pressure deficit (VPD) levels when incoming short-wave radiation (R_{si}) is sufficiently high (i.e., $R_{si} \geq 400$ W/m^2) during the growing season (May, June, July, and August) for all the six paired sites (a–f). Note that the samples are binned by VPD for every 0.2 kPa. Δ*LE* is mostly positive across sites, while Δ*H* is mostly positive except for DK-Broadleaf site. AR, Arkansas; CW, Coweeta; DK-Broadleaf, Duke Forest-Hardwood; DK-Needleleaf, Duke Forest-Loblolly Pine; IN, Indiana; NH, New Hampshire [Colour figure can be viewed at wileyonlinelibrary.com]

influenced by differences in *H* between the forests and grasslands, which increased as a function of VPD in at least two sites (IN and CW, Figure 9b,c). Albedo, emissivity, and incoming radiation did not depend on VPD within or across sites; however, the imbalance term tended to decrease as VPD increased in most sites (Figure 9). Finally, we note that the relationships between $\Delta T_{s,obs}$ and VPD are similar to the relationships between $\Delta T_{s,obs}$ and surface temperature itself (Figure S7), reflecting the strong covariation between VPD and temperature.

4 | DISCUSSION

Previous research has established that reforestation tends to have a surface cooling effect in the tropical zone, driven largely by enhanced evapotranspiration by forests (Bonan, 2008). In contrast, in the boreal zone, reforestation can have a warming effect driven largely by lower forest albedo compared with the snow-covered grasslands (Lee et al., 2011; Swann et al., 2010). However, investigations of how reforestation impacts surface temperature in the temperate zone have historically lacked generality (Lejeune et al., 2018), though forest warming has been demonstrated in winter for seasonally snow-covered lands in the eastern United States (Burakowski et al., 2018). By using remote sensing data or coupled climate-land surface models, both forest cooling (Alkama & Cescatti, 2016; Bright et al., 2017; Jackson et al., 2005; Ramankutty et al., 2006; Wickham et al., 2013) and warming (Feddema et al., 2005; Hansen et al., 1998) effects ΔT_s were reported.

Our study leveraged comprehensive in-situ observations in investigating not only when, but also why, land cover affects surface temperature over a wide range of latitudes in the temperate zone. At the annual time scale, the surface of forests was 1–2°C cooler than grasslands, with substantially larger cooling observed during the growing season (Figure 5), and when VPD is elevated (Figure 8). This conclusion is drawn by comparing not only direct observations of radiometric surface temperature ($\Delta T_{s,obs}$) but also by calculating the expected T_s changes considering all of the components of the ecosystem energy balance ($\Delta T_{s,cal}$). Across sites, the observed and calculated ΔT_s agreed well (Figures S2 and S3).

In most sites, the forest cooling effect persists throughout the year, but is driven by different mechanisms depending on the season. Specifically, enhanced forest evapotranspiration is a strong determinant of surface temperature difference during the growing season, whereas in the dormant season, enhanced forest sensible heat flux plays a stronger role (Figure 5). As expected, decreased albedo over forests led to warming (Figure 5); however, this warming was offset somewhat by increased forest emissivity and was not sufficiently large to balance cooling from other terms of the surface energy balance. Our results are consistent with those reported in preceding work (Alkama & Cescatti, 2016; Bright et al., 2017; Burakowski et al., 2018; Juang et al., 2007; Wickham et al., 2013); however, our study is the first to link surface temperature differences to observed energy cycle pools and fluxes measured across a wide range of latitudes.

4.1 | The seasonal variations in the components of the ΔT_s

At most sites, the ΔT_s between forests and grasslands was more pronounced during the growing season and generally less pronounced during winter (Figure 4). However, the seasonal variations in the contributing components were less generalizable across sites. The contributions of albedo (Figure S8) and emissivity (Figure S9) at most sites were more pronounced outside of the growing season. Differences in albedo between forests and grasslands may be relatively small during the growing season (i.e., darker green versus lighter green). In contrast, during winter, grasslands are often covered by dormant vegetation or snow, which both have higher albedo (Betts & Ball, 1997; Burakowski et al., 2015; Wang et al., 2014) than forests in winter due to canopy masking of snow under forest canopies and the lower albedo of evergreen species at some sites (i.e., CW and AR) if snow is not present on the tree canopy.

Sensible and latent heat flux contributions to ΔT_s followed the seasonal patterns of the phenological cycle, reflecting their dependence on surface vegetation and associated ecophysiological processes (Juang et al., 2007). At almost all sites, the relatively higher *LE* from forests tended to cool the surface during the growing season, but not during other parts of the year (Figure S10). In contrast to *LE*, a decrease in growing season *H* from forests tends to warm the surface (Figure S11), but during other parts of the year, the higher *H* from forests cool the surface, on average. During the growing season, the pronounced contribution of *LE* to ΔT_s reflects higher G_s (Figure 6, right column) over forests than grasslands. During the other times of the year, the pronounced contribution of *H* to ΔT_s reflects larger differences in turbulent mixing resulting from a bigger difference in g_a between bare trees and grasses (Figure 6, middle column).

The contribution of incoming radiation to the ΔT_s varied across sites (Figure S12), though it was close to 0°C for most sites (e.g., NH, IN, CW, and AR). For DK-Needleleaf and DK-Broadleaf, R_i was almost consistently lower over forests, which may reflect a bias in the upward facing net radiation sensors or perhaps local effects of greater aerosol production in forests, although this cannot be determined using available measurements. *G* was not measured at all sites, and it had no clear seasonal impact on ΔT_s in sites where it was measured (Figure S13). The contribution of the residual of the energy balance (*I*) does not show consistent patterns across sites (Figure S14), suggesting that missing energy flux terms can be excluded as a dominant explanation for differences in ΔT_s. This is consistent with findings that forests and non-forested ecosystems do not differ in energy balance closure on average (Stoy et al., 2013).

4.2 | The effect of reforestation on surface temperature under changing hydro-climatic conditions

In most of the paired sites, the cooling effect of forests was most pronounced during periods characterized by high VPD and high surface temperature (Figure 8; Figure S7). It should be noted that because VPD and air temperature are highly correlated, this result can also be interpreted as a greater cooling effect of forests when temperature is especially high.

During periods of hydrologic stress, forests tend to maintain a relatively higher evapotranspiration compared with grasslands (Stoy et al., 2006; Teuling et al., 2010; Wang, Fu, Gao, Yao, & Zhou, 2012), reflecting the combined effects of greater leaf area, greater reliance on stored water in plant tissue (Matheny et al., 2014; Zhang, Manzoni, Katul, Porporato, & Yang, 2014), and greater rooting depth (Tanaka et al., 2004). In half of our study sites (NH, DK-Broadleaf, and AR), the enhanced cooling of forests during high VPD periods can be linked to enhanced evapotranspiration in the forests (Figure 9). However, in other sites, patterns are less clear and confounded by VPD-driven difference in sensible heat flux, and the energy imbalance term. Moreover, in many sites, canopy surface conductance declined more rapidly within increasing VPD in the forests when compared to the paired grasslands (Figure S6).

Our results suggest that the surface cooling effect of reforestation in the temperate eastern United States is generally greatest when VPD, and temperature, are highest—consistent with other work suggesting that forest cover can modulate the occurrence of temperature extremes (LeJeune et al., 2018). Ultimately, however, our efforts to link the relationship between ΔT_s and VPD to mechanistic responses to hydrologic stress are limited by the fact that our study period contained relatively few drought events. VPD is already rising across much of the conterminous United States (Ficklin & Novick, 2017; Zhang et al., 2019), driven by increases in saturated vapor pressure that are not matched by concurrent increases in actual vapor pressure, and a further increase in global temperature will further drive more frequent and severe hydrologic stress (Park et al., 2018). Thus, further work to understand how the climate mitigation potential of reforestation depends on hydrologic state is clearly needed.

4.3 | Limitations of this study and directions for future research

By providing information on all the terms of the ecosystem energy budget, EC flux towers are a useful tool for quantifying not only if reforestation offers a local cooling benefit but also when and why. However, flux tower measurements are sensitive to a number of well-documented random and systematic uncertainties, including a pervasive lack of energy balance closure (Foken, 2008; Stoy et al., 2013). In this study, the lack of energy balance closure amounted to a slight warming effect over forests (see Figure 5). Thus, while this particular shortcoming of EC systems does not fundamentally change our conclusions, it does impact the precision with which we can attribute the cooling potential of reforestation to specific mechanism. Our conclusions are also limited to some extent by the number of study sites considered; certainly, questions like those pursued in our study would benefit from more micro-clusters of flux towers located in sites that experience similar macroclimate but different land cover. Results may also be sensitive to the model used to estimate ecosystem-scale emissivity (e.g., the model of Juang et al., 2007), which is commonly used but ultimately based on relatively few observations. Angular effects on emissivity are negligible in vegetated canopies (Sobrino, Jimenez-Munoz, & Verhoef, 2005) so we assume that sensor placement does not impact emissivity estimates. We also repeated our analysis assuming that emissivity was always equal to 1, and found our results did not change appreciably (results not shown). Nonetheless, future work exploring LUCC effects on surface temperature would benefit from new approaches to describe how the emissivity varies in relationship to albedo across the landscape and with time. Future work leveraging remotely sensed observations of surface temperature (e.g., from MODIS) would enhance the generalizability of our results across broad eco-climatic gradients (Alkama & Cescatti, 2016) although site-level

micrometeorological measurements would remain necessary to determine the factors that drive the T_s differences.

This particular study is exclusively focused on how reforestation affects surface temperature. Surface temperature is a critical variable for a range of ecological processes, including respiration (Reichstein et al., 2003), photosynthesis (Bernacchi, Singsaas, Pimentel, Portis, & Long, 2001), and ontogeny (Thuiller, Lavorel, Araujo, Sykes, & Prentice, 2005). However, spatial and temporal variation in surface temperature may not necessarily be coupled to variation in air temperature, which is an important climate system variable (Winckler et al., 2019). Since *H* transfers heat from the surface to the atmosphere, ecosystems with relatively cool surfaces may underlie relatively warm air (Baldocchi & Ma, 2013), and vice versa. These dynamics are further mediated by land-cover-driven changes in the height of the planetary boundary layer (Luyssaert et al., 2014), which is generally greater over forests, creating more "room" for heat energy transferred from the surface to the atmosphere. These dynamics are further complicated by the fact that flux towers over forests typically measure fluxes within the roughness sublayer, where canopy structure greatly affects the near-surface temperature gradient (Harman & Finnigan, 2008). While outside the scope of this particular study, we point readers to Novick and Katul (2020) for a complimentary analysis of the extent to which LUCC modifications to surface temperature extend to differences in air temperature across the atmospheric mixed layer.

5 | CONCLUSION

Here, we show that the surface of temperate forests is generally cooler than grasslands in the temperate zone, especially during the growing season and periods of hydrologic stress. This result provides much needed observational evidence for the direct climate mitigation benefits of reforestation across the temperate zone that previously had been limited to numerical model and remote sensing studies. In particular, this study applies in-situ field observations by using 11 flux towers that span a wide range of latitudes at five sites in the temperate zone of the eastern United States to explain the mechanisms underlying temperature differences between forests and grasslands. Our results showed that the surface of forests is 1–2°C cooler than grasslands. The albedo warming effect is pronounced across sites (+2.3°C on average), though offset by the emissivity cooling effect (−0.8°C on average). The enhanced turbulent fluxes of latent heat and sensible heat of forests have a combined cooling effect (−2.5°C on average) that further offsets the albedo warming effect. On the annual scale, the evaporative cooling effect is less important than expected, perhaps because the wet conditions in the mesic eastern United States tend to prevent moisture limitations to latent heat flux most of the time. However, our results suggest that latent heat flux-driven cooling may become more important in the future, when VPD is projected to be generally higher and more drought-like conditions could prevail (Ficklin & Novick, 2017). The sensible heat flux is a dominant contributor to the surface temperature difference between forests and grasslands, where the higher aerodynamic conductance of forests outweighs the greater surface–air temperature difference in determining the sensible heat flux.

ACKNOWLEDGEMENTS

K.A.N. acknowledges support from NSF-DEB grants 1552747 and 1637522, and NASA-ROSES grant NNX17AE69G. Q.Z. acknowledges the support from NSFC-NSF collaboration (P. R. China-U.S.) funding number 51861125102. P.C.S. acknowledges support from the US National Science Foundation award numbers 1552976, 1241881, and 1702029 and the USDA National Institute of Food and Agriculture Hatch project 228396 and Multi-State project W3188. E.B. acknowledges support from NSF-DEB #1802726 and NSF-EPSCoR RII Track-4 #1832959, and NSF-EPSCoR RII Track 2 #1920908. The IN sites are supported by the AmeriFlux Management Project, administered by the US Department of Energy. The NH sites are supported by USDA National Institute of Food and Agriculture Hatch project 1006997 and by the US National Science Foundation through the NH EPSCoR Ecosystem and Society Project (NSF-EPS 1101245). The CW forest site is supported by the USDA Forest Service, Southern Research Station; US EPA agreement number 13-IA-11330140-044, USDA NIFA Agriculture and Food Research Initiative Foundational Program award number 2012-67019-19484; NSF-LTER program, award #DEB-0823293 and #DEB-1440485. The authors declare no conflict of interest.

DATA AVAILABILITY STATEMENT

The AmeriFlux sites used in this study are accessible at https://ameriflux.lbl.gov/; other sites are to be shared with AmeriFlux when finishing the site registrations, at the current stage the data are available by contacting the author of correspondence.

ORCID

Quan Zhang https://orcid.org/0000-0003-1127-5969
A. Christopher Oishi https://orcid.org/0000-0001-5064-4080
Rebecca Sanders-DeMott https://orcid.org/0000-0002-0709-8042
Koong Yi https://orcid.org/0000-0002-8630-3031
Kimberly A. Novick https://orcid.org/0000-0002-8431-0879

REFERENCES

Alkama, R., & Cescatti, A. (2016). Biophysical climate impacts of recent changes in global forest cover. *Science*, *351*(6273), 600–604. https://doi.org/10.1126/science.aac8083

Anderson-Teixeira, K. J., Snyder, P. K., Twine, T. E., Cuadra, S. V., Costa, M. H., & Delucia, E. H. (2012). Climate-regulation services of natural and agricultural ecoregions of the Americas. *Nature Climate Change*, *2*, 177–181. https://doi.org/10.1038/Nclimate1346

Baldocchi, D., Falge, E., Gu, L., Olson, R., Hollinger, D., Running, S., … Evans, R. (2001). FLUXNET: A new tool to study the temporal and spatial variability of ecosystem-scale carbon dioxide, water vapor, and energy flux densities. *Bulletin of the American Meteorological Society*, *82*(11), 2415–2434. https://doi.org/10.1175/1520-0477

Baldocchi, D., & Ma, S. Y. (2013). How will land use affect air temperature in the surface boundary layer? Lessons learned from a comparative study on the energy balance of an oak savanna and annual grassland

in California, USA. *Tellus Series B-Chemical and Physical Meteorology*, *65*. https://doi.org/10.3402/tellusb.v65i0.19994

Banerjee, T., De Roo, F., & Mauder, M. (2017). Explaining the convector effect in canopy turbulence by means of large-eddy simulation. *Hydrology and Earth System Sciences*, *21*(6), 2987–3000. https://doi.org/10.5194/hess-21-2987-2017

Barry, R. (1970). A framework for climatological research with particular reference to scale concepts. *Transactions of the Institute of British Geographers*, 61–70. https://doi.org/10.2307/621641

Bastin, J.-F., Finegold, Y., Garcia, C., Mollicone, D., Rezende, M., Routh, D., … Crowther, T. W. (2019). The global tree restoration potential. *Science*, *365*(6448), 76–79. https://doi.org/10.1126/science.aax0848

Bernacchi, C. J., Singsaas, E. L., Pimentel, C., Portis, A. R., & Long, S. P. (2001). Improved temperature response functions for models of Rubisco-limited photosynthesis. *Plant Cell and Environment*, *24*(2), 253–259. https://doi.org/10.1111/j.1365-3040.2001.00668.x

Betts, A. K., & Ball, J. H. (1997). Albedo over the boreal forest. *Journal of Geophysical Research-Atmospheres*, *102*(D24), 28901–28909. https://doi.org/10.1029/96jd03876

Bonan, G. B. (2008). Forests and climate change: Forcings, feedbacks, and the climate benefits of forests. *Science*, *320*(5882), 1444–1449. https://doi.org/10.1126/science.1155121

Bonan, G. B. (2016). Forests, climate, and public policy: A 500-year interdisciplinary odyssey. *Annual Review of Ecology, Evolution, and Systematics*, *47*, 97–121. https://doi.org/10.1146/annurev-ecolsys-121415-032359

Boyd, M. A., Berner, L. T., Doak, P., Goetz, S. J., Rogers, B. M., Wagner, D., … Mack, M. C. (2019). Impacts of climate and insect herbivory on productivity and physiology of trembling aspen (*Populus tremuloides*) in Alaskan boreal forests. *Environmental Research Letters*, *14*(8). https://doi.org/10.1088/1748-9326/ab215f

Bright, R. M., Davin, E., O'Halloran, T., Pongratz, J., Zhao, K. G., & Cescatti, A. (2017). Local temperature response to land cover and management change driven by non-radiative processes. *Nature Climate Change*, *7*(4), 296–302. https://doi.org/10.1038/Nclimate3250

Buotte, P. C., Levis, S., Law, B. E., Hudiburg, T. W., Rupp, D. E., & Kent, J. J. (2019). Near-future forest vulnerability to drought and fire varies across the western United States. *Global Change Biology*, *25*(1), 290–303. https://doi.org/10.1111/gcb.14490

Burakowski, E. A., Ollinger, S. V., Lepine, L., Schaaf, C. B., Wang, Z., Dibb, J. E., … Martin, M. (2015). Spatial scaling of reflectance and surface albedo over a mixed-use, temperate forest landscape during snow-covered periods. *Remote Sensing of Environment*, *158*, 465–477. https://doi.org/10.1016/j.rse.2014.11.023

Burakowski, E., Tawfik, A., Ouimette, A., Lepine, L., Novick, K., Ollinger, S., … Bonan, G. (2018). The role of surface roughness, albedo, and Bowen ratio on ecosystem energy balance in the Eastern United States. *Agricultural and Forest Meteorology*, *249*, 367–376. https://doi.org/10.1016/j.agrformet.2017.11.030

Cook, B. I., Ault, T. R., & Smerdon, J. E. (2015). Unprecedented 21st century drought risk in the American Southwest and Central Plains. *Science Advances*, *1*(1). https://doi.org/10.1126/sciadv.1400082

Costa, M. (2005). Large-scale hydrological impacts of tropical forest conversion. In M. Bonell & L. Bruijnzeel (Eds.), *Forests, water and people in the humid tropics: Past, present and future hydrological research for integrated land and water management*. International Hydrology Series (pp. 590–597). Cambridge: Cambridge University Press. https://doi.org/10.1017/CBO9780511535666.030

Eder, F., Schmidt, M., Damian, T., Traumner, K., & Mauder, M. (2015). Mesoscale eddies affect near-surface turbulent exchange: Evidence from Lidar and tower measurements. *Journal of Applied Meteorology and Climatology*, *54*(1), 189–206. https://doi.org/10.1175/Jamc-D-14-0140.1

Feddema, J. J., Oleson, K. W., Bonan, G. B., Mearns, L. O., Buja, L. E., Meehl, G. A., & Washington, W. M. (2005). The importance of land-cover change in simulating future climates. *Science*, *310*(5754), 1674–1678. https://doi.org/10.1126/science.1118160

Ficklin, D. L., & Novick, K. A. (2017). Historic and projected changes in vapor pressure deficit suggest a continental-scale drying of the United States atmosphere. *Journal of Geophysical Research-Atmospheres*, *122*(4), 2061–2079. https://doi.org/10.1002/2016jd025855

Foken, T. (2008). The energy balance closure problem: An overview. *Ecological Applications*, *18*(6), 1351–1367. https://doi.org/10.1890/06-0922.1

Foley, J. A., Costa, M. H., Delire, C., Ramankutty, N., & Snyder, P. (2003). Green surprise? How terrestrial ecosystems could affect earth's climate. *Frontiers in Ecology and the Environment*, *1*(1), 38–44. https://doi.org/10.1890/1540-9295

Frank, D., Reichstein, M., Bahn, M., Thonicke, K., Frank, D., Mahecha, M. D., … Zscheischler, J. (2015). Effects of climate extremes on the terrestrial carbon cycle: Concepts, processes and potential future impacts. *Global Change Biology*, *21*(8), 2861–2880. https://doi.org/10.1111/gcb.12916

Fratini, G., Ibrom, A., Arriga, N., Burba, G., & Papale, D. (2012). Relative humidity effects on water vapour fluxes measured with closed-path eddy-covariance systems with short sampling lines. *Agricultural and Forest Meteorology*, *165*, 53–63. https://doi.org/10.1016/j.agrformet.2012.05.018

Goldewijk, K. K. (2001). Estimating global land use change over the past 300 years: The HYDE Database. *Global Biogeochemical Cycles*, *15*(2), 417–433. https://doi.org/10.1029/1999gb001232

Green, J. K., Seneviratne, S. I., Berg, A. M., Findell, K. L., Hagemann, S., Lawrence, D. M., & Gentine, P. (2019). Large influence of soil moisture on long-term terrestrial carbon uptake. *Nature*, *565*(7740), 476–479. https://doi.org/10.1038/s41586-018-0848-x

Hall, B., Motzkin, G., Foster, D. R., Syfert, M., & Burk, J. (2002). Three hundred years of forest and land-use change in Massachusetts, USA. *Journal of Biogeography*, *29*(10–11), 1319–1335. https://doi.org/10.1046/j.1365-2699.2002.00790.x

Hansen, J. E., Sato, M., Lacis, A., Ruedy, R., Tegen, I., & Matthews, E. (1998). Climate forcings in the industrial era. *Proceedings of the National Academy of Sciences of the United States of America*, *95*(22), 12753–12758. https://doi.org/10.1073/pnas.95.22.12753

Harman, I. N., & Finnigan, J. J. (2008). Scalar concentration profiles in the canopy and roughness sublayer. *Boundary-Layer Meteorology*, *129*(3), 323–351. https://doi.org/10.1007/s10546-008-9328-4

Hooker, T. D., & Compton, J. E. (2003). Forest ecosystem carbon and nitrogen accumulation during the first century after agricultural abandonment. *Ecological Applications*, *13*(2), 299–313. https://doi.org/10.1890/1051-0761

Houghton, R. A., Hackler, J. L., & Lawrence, K. T. (1999). The US carbon budget: Contributions from land-use change. *Science*, *285*(5427), 574–578. https://doi.org/10.1126/science.285.5427.574

House, J. I., Prentice, I. C., & Le Quere, C. (2002). Maximum impacts of future reforestation or deforestation on atmospheric CO_2. *Global Change Biology*, *8*(11), 1047–1052. https://doi.org/10.1046/j.1365-2486.2002.00536.x

Huang, L., Zhai, J., Liu, J., & Sun, C. (2018). The moderating or amplifying biophysical effects of afforestation on CO_2-induced cooling depend on the local background climate regimes in China. *Agricultural and Forest Meteorology*, *260*, 193–203. https://doi.org/10.1016/j.agrformet.2018.05.020

Jackson, R. B., Jobbagy, E. G., Avissar, R., Roy, S. B., Barrett, D. J., Cook, C. W., … Murray, B. C. (2005). Trading water for carbon with biological sequestration. *Science*, *310*(5756), 1944–1947. https://doi.org/10.1126/science.1119282

Juang, J. Y., Katul, G., Siqueira, M., Stoy, P., & Novick, K. (2007). Separating the effects of albedo from eco-physiological changes on surface temperature along a successional chronosequence in the

southeastern United States. *Geophysical Research Letters*, *34*(21). https://doi.org/10.1029/2007gl031296

Jung, M., Reichstein, M., Ciais, P., Seneviratne, S. I., Sheffield, J., Goulden, M. L., … Zhang, K. E. (2010). Recent decline in the global land evapotranspiration trend due to limited moisture supply. *Nature*, *467*(7318), 951–954. https://doi.org/10.1038/nature09396

Kelliher, F. M., Leuning, R., & Schulze, E. D. (1993). Evaporation and canopy characteristics of coniferous forests and grasslands. *Oecologia*, *95*(2), 153–163. https://doi.org/10.1007/Bf00323485

Kim, J., & Verma, S. B. (1991). Modeling canopy stomatal conductance in a temperate grassland ecosystem. *Agricultural and Forest Meteorology*, *55*(1–2), 149–166. https://doi.org/10.1016/0168-1923(91)90028-O

Konings, A. G., Williams, A. P., & Gentine, P. (2017). Sensitivity of grassland productivity to aridity controlled by stomatal and xylem regulation. *Nature Geoscience*, *10*(4), 284–288. https://doi.org/10.1038/Ngeo2903

Law, B. E., Hudiburg, T. W., Berner, L. T., Kent, J. J., Buotte, P. C., & Harmon, M. E. (2018). Land use strategies to mitigate climate change in carbon dense temperate forests. *Proceedings of the National Academy of Sciences of the United States of America*, *115*(14), 3663–3668. https://doi.org/10.1073/pnas.1720064115

Lee, X., Goulden, M. L., Hollinger, D. Y., Barr, A., Black, T. A., Bohrer, G., … Zhao, L. (2011). Observed increase in local cooling effect of deforestation at higher latitudes. *Nature*, *479*(7373), 384–387. https://doi.org/10.1038/nature10588

Lejeune, Q., Davin, E. L., Gudmundsson, L., Winckler, J., & Seneviratne, S. I. (2018). Historical deforestation locally increased the intensity of hot days in northern mid-latitudes. *Nature Climate Change*, *8*(5), 386–390. https://doi.org/10.1038/s41558-018-0131-z

Lemordant, L., Gentine, P., Swann, A. S., Cook, B. I., & Scheff, J. (2018). Critical impact of vegetation physiology on the continental hydrologic cycle in response to increasing CO_2. *Proceedings of the National Academy of Sciences of the United States of America*, *115*(16), 4093–4098. https://doi.org/10.1073/pnas.1720712115

Li, X. I., Gentine, P., Lin, C., Zhou, S., Sun, Z., Zheng, Y. I., … Zheng, C. (2019). A simple and objective method to partition evapotranspiration into transpiration and evaporation at eddy-covariance sites. *Agricultural and Forest Meteorology*, *265*, 171–182. https://doi.org/10.1016/j.agrformet.2018.11.017

Liu, Z. J., Liu, Y. S., & Baig, M. H. A. (2019). Biophysical effect of conversion from croplands to grasslands in water-limited temperate regions of China. *Science of the Total Environment*, *648*, 315–324. https://doi.org/10.1016/j.scitotenv.2018.08.128

Luyssaert, S., Jammet, M., Stoy, P. C., Estel, S., Pongratz, J., Ceschia, E., … Dolman, A. J. (2014). Land management and land-cover change have impacts of similar magnitude on surface temperature. *Nature Climate Change*, *4*(5), 389–393. https://doi.org/10.1038/Nclimate2196

Manson, S. M., & Evans, T. (2007). Agent-based modeling of deforestation in southern Yucatan, Mexico, and reforestation in the Midwest United States. *Proceedings of the National Academy of Sciences of the United States of America*, *104*(52), 20678–20683. https://doi.org/10.1073/pnas.0705802104

Matheny, A. M., Bohrer, G., Stoy, P. C., Baker, I. T., Black, A. T., Desai, A. R., … Verbeeck, H. (2014). Characterizing the diurnal patterns of errors in the prediction of evapotranspiration by several land-surface models: An NACP analysis. *Journal of Geophysical Research-Biogeosciences*, *119*(7), 1458–1473. https://doi.org/10.1002/2014jg002623

Mather, A. S. (1992). The forest transition. *Area*, *24*(4), 367–379.

Monteith, J. L. (1965). *Evaporation and environment*. Paper presented at the Symposia of the Society for Experimental Biology.

Monteith, J. L., & Unsworth, M. H. (1990). *Principles of environmental physics* (2nd ed.). London, New York: E. Arnold. Distributed in the USA by Routledge, Chapman and Hall.

Novick, K. A., Biederman, J. A., Desai, A. R., Litvak, M. E., Moore, D. J. P., Scott, R. L., & Torn, M. S. (2018). The AmeriFlux network: A coalition of the willing. *Agricultural and Forest Meteorology*, *249*, 444–456. https://doi.org/10.1016/j.agrformet.2017.10.009

Novick, K. A., Ficklin, D. L., Stoy, P. C., Williams, C. A., Bohrer, G., Oishi, A. C., … Phillips, R. P. (2016). The increasing importance of atmospheric demand for ecosystem water and carbon fluxes. *Nature Climate Change*, *6*(11), 1023–1027. https://doi.org/10.1038/Nclimate3114

Novick, K. A., & Katul, G. G. (2020). Reforestation and duality between surface and air temperature. *Journal of Geophysical Research – Biogeosciences*. https://doi.org/10.1029/2019JG005543

Novick, K. A., Oishi, A. C., Ward, E. J., Siqueira, M. B. S., Juang, J. Y., & Stoy, P. C. (2015). On the difference in the net ecosystem exchange of CO_2 between deciduous and evergreen forests in the southeastern United States. *Global Change Biology*, *21*(2), 827–842. https://doi.org/10.1111/gcb.12723

Novick, K. A., Stoy, P. C., Katul, G. G., Ellsworth, D. S., Siqueira, M. B. S., Juang, J., & Oren, R. (2004). Carbon dioxide and water vapor exchange in a warm temperate grassland. *Oecologia*, *138*(2), 259–274. https://doi.org/10.1007/s00442-003-1388-z

Novick, K., Walker, J., Chan, W., Schmidt, A., Sobek, C., & Vose, J. (2013). Eddy covariance measurements with a new fast-response, enclosed-path analyzer: Spectral characteristics and cross-system comparisons. *Agricultural and Forest Meteorology*, *181*, 17–32. https://doi.org/10.1016/j.agrformet.2013.06.020

Ocheltree, T. W., & Loescher, H. W. (2007). Design of the AmeriFlux portable eddy covariance system and uncertainty analysis of carbon measurements. *Journal of Atmospheric and Oceanic Technology*, *24*(8), 1389–1406. https://doi.org/10.1175/Jtech2064.1

Oishi, A. C., Miniat, C. F., Novick, K. A., Brantle, S. T., Vose, J. M., & Walker, J. T. (2018). Warmer temperatures reduce net carbon uptake, but do not affect water use, in a mature southern Appalachian forest. *Agricultural and Forest Meteorology*, *252*, 269–282. https://doi.org/10.1016/j.agrformet.2018.01.011

Pan, Y., Birdsey, R. A., Fang, J., Houghton, R., Kauppi, P. E., Kurz, W. A., … Hayes, D. (2011). A large and persistent carbon sink in the world's forests. *Science*, *333*(6045), 988–993. https://doi.org/10.1126/science.1201609

Papale, D., Reichstein, M., Aubinet, M., Canfora, E., Bernhofer, C., Kutsch, W., … Yakir, D. (2006). Towards a standardized processing of Net Ecosystem Exchange measured with eddy covariance technique: Algorithms and uncertainty estimation. *Biogeosciences*, *3*(4), 571–583. https://doi.org/10.5194/bg-3-571-2006

Park, C. E., Jeong, S. J., Joshi, M., Osborn, T. J., Ho, C. H., Piao, S. L., … Feng, S. (2018). Keeping global warming within 1.5 degrees C constrains emergence of aridification. *Nature Climate Change*, *8*(1), 70–74. https://doi.org/10.1038/s41558-017-0034-4

Peng, S.-S., Piao, S., Zeng, Z., Ciais, P., Zhou, L., Li, L. Z. X., … Zeng, H. (2014). Afforestation in China cools local land surface temperature. *Proceedings of the National Academy of Sciences of the United States of America*, *111*, 2915–2919. https://doi.org/10.1073/pnas.1315126111

Pielke, R. A., Avissar, R. I., Raupach, M., Dolman, A. J., Zeng, X., & Denning, A. S. (1998). Interactions between the atmosphere and terrestrial ecosystems: Influence on weather and climate. *Global Change Biology*, *4*(5), 461–475. https://doi.org/10.1046/j.1365-2486.1998.t01-1-00176.x

Porporato, A., Laio, F., Ridolfi, L., & Rodriguez-Iturbe, I. (2001). Plants in water-controlled ecosystems: Active role in hydrologic processes and response to water stress – III. Vegetation water stress. *Advances in Water Resources*, *24*(7), 725–744. https://doi.org/10.1016/S0309-1708(01)00006-9

Ramankutty, N., Delire, C., & Snyder, P. (2006). Feedbacks between agriculture and climate: An illustration of the potential unintended consequences of human land use activities. *Global and Planetary Change*, *54*(1–2), 79–93. https://doi.org/10.1016/j.gloplacha.2005.10.005

Ramankutty, N., Heller, E., & Rhemtulla, J. (2010). Prevailing myths about agricultural abandonment and forest regrowth in the United States.

Annals of the Association of American Geographers, *100*(3), 502–512. https://doi.org/10.1080/00045601003788876

Reichstein, M., Rey, A., Freibauer, A., Tenhunen, J., Valentini, R., Banza, J., … Yakir, D. (2003). Modeling temporal and large-scale spatial variability of soil respiration from soil water availability, temperature and vegetation productivity indices. *Global Biogeochemical Cycles*, *17*(4). https://doi.org/10.1029/2003gb002035

Rigden, A. J., & Li, D. (2017). Attribution of surface temperature anomalies induced by land use and land cover changes. *Geophysical Research Letters*, *44*(13), 6814–6822. https://doi.org/10.1002/2017gl073811

Rigden, A. J., & Salvucci, G. D. (2017). Stomatal response to humidity and CO_2 implicated in recent decline in US evaporation. *Global Change Biology*, *23*(3), 1140–1151. https://doi.org/10.1111/gcb.13439

Rudel, T. K., Coomes, O. T., Moran, E., Achard, F., Angelsen, A., Xu, J. C., & Lambin, E. (2005). Forest transitions: Towards a global understanding of land use change. *Global Environmental Change-Human and Policy Dimensions*, *15*(1), 23–31. https://doi.org/10.1016/j.gloenvcha.2004.11.001

Schultz, N. M., Lawrence, P. J., & Lee, X. H. (2017). Global satellite data highlights the diurnal asymmetry of the surface temperature response to deforestation. *Journal of Geophysical Research-Biogeosciences*, *122*(4), 903–917. https://doi.org/10.1002/2016jg003653

Sobrino, J. A., Jimenez-Munoz, J. C., & Verhoef, W. (2005). Canopy directional emissivity: Comparison between models. *Remote Sensing of Environment*, *99*(3), 304–314. https://doi.org/10.1016/j.rse.2005.09.005

Stoy, P. C., Katul, G. G., Siqueira, M. B. S., Juang, J.-Y., Novick, K. A., McCarthy, H. R., … Oren, R. (2006). Separating the effects of climate and vegetation on evapotranspiration along a successional chronosequence in the southeastern US. *Global Change Biology*, *12*(11), 2115–2135. https://doi.org/10.1111/j.1365-2486.2006.01244.x

Stoy, P. C., Katul, G. G., Siqueira, M. B. S., Juang, J.-Y., Novick, K. A., McCarthy, H. R., … Oren, R. (2008). Role of vegetation in determining carbon sequestration along ecological succession in the southeastern United States. *Global Change Biology*, *14*(6), 1409–1427. https://doi.org/10.1111/j.1365-2486.2008.01587.x

Stoy, P. C., Mauder, M., Foken, T., Marcolla, B., Boegh, E., Ibrom, A., … Varlagin, A. (2013). A data-driven analysis of energy balance closure across FLUXNET research sites: The role of landscape scale heterogeneity. *Agricultural and Forest Meteorology*, *171*, 137–152. https://doi.org/10.1016/j.agrformet.2012.11.004

Sulman, B. N., Roman, D. T., Scanlon, T. M., Wang, L. X., & Novick, K. A. (2016). Comparing methods for partitioning a decade of carbon dioxide and water vapor fluxes in a temperate forest. *Agricultural and Forest Meteorology*, *226*, 229–245. https://doi.org/10.1016/j.agrformet.2016.06.002

Sulman, B. N., Roman, D. T., Yi, K., Wang, L. X., Phillips, R. P., & Novick, K. A. (2016). High atmospheric demand for water can limit forest carbon uptake and transpiration as severely as dry soil. *Geophysical Research Letters*, *43*(18), 9686–9695. https://doi.org/10.1002/2016gl069416

Swann, A. L., Fung, I. Y., Levis, S., Bonan, G. B., & Doney, S. C. (2010). Changes in Arctic vegetation amplify high-latitude warming through the greenhouse effect. *Proceedings of the National Academy of Sciences of the United States of America*, *107*(4), 1295–1300. https://doi.org/10.1073/pnas.0913846107

Tanaka, K., Takizawa, H., Kume, T., Xu, J. Q., Tantasirin, C., & Suzuki, M. (2004). Impact of rooting depth and soil hydraulic properties on the transpiration peak of an evergreen forest in northern Thailand in the late dry season. *Journal of Geophysical Research-Atmospheres*, *109*(D23). https://doi.org/10.1029/2004jd004865

Teuling, A. J., Seneviratne, S. I., Stöckli, R., Reichstein, M., Moors, E., Ciais, P., … Wohlfahrt, G. (2010). Contrasting response of European forest and grassland energy exchange to heatwaves. *Nature Geoscience*, *3*(10), 722–727. https://doi.org/10.1038/Ngeo950

Thuiller, W., Lavorel, S., Araujo, M. B., Sykes, M. T., & Prentice, I. C. (2005). Climate change threats to plant diversity in Europe. *Proceedings of the National Academy of Sciences of the United States of America*, *102*(23), 8245–8250. https://doi.org/10.1073/pnas.0409902102

van Beek, L. P. H., Wada, Y., & Bierkens, M. F. P. (2011). Global monthly water stress: 1. Water balance and water availability. *Water Resources Research*, *47*. https://doi.org/10.1029/2010wr009791

van der Werf, G. R., Morton, D. C., DeFries, R. S., Olivier, J. G. J., Kasibhatla, P. S., Jackson, R. B., … Randerson, J. T. (2009). CO_2 emissions from forest loss. *Nature Geoscience*, *2*(11), 737–738. https://doi.org/10.1038/ngeo671

Vick, E. S. K., Stoy, P. C., Tang, A. C. I., & Gerken, T. (2016). The surface-atmosphere exchange of carbon dioxide, water, and sensible heat across a dryland wheat-fallow rotation. *Agriculture Ecosystems & Environment*, *232*, 129–140. https://doi.org/10.1016/j.agee.2016.07.018

Wang, S., Fu, B. J., Gao, G. Y., Yao, X. L., & Zhou, J. (2012). Soil moisture and evapotranspiration of different land cover types in the Loess Plateau. *China. Hydrology and Earth System Sciences*, *16*(8), 2883–2892. https://doi.org/10.5194/hess-16-2883-2012

Wang, Z., Schaaf, C. B., Strahler, A. H., Chopping, M. J., Román, M. O., Shuai, Y., … Fitzjarrald, D. R. (2014). Evaluation of MODIS albedo product (MCD43A) over grassland, agriculture and forest surface types during dormant and snow-covered periods. *Remote Sensing of Environment*, *140*, 60–77. https://doi.org/10.1016/j.rse.2013.08.025

Wear, D. N., & Greis, J. G. (2012). *The southern forest futures project: Summary report* (Vol. *168*, pp. 1–54). *Gen. Tech. Rep. SRS-GTR-168*. Asheville, NC: USDA-Forest Service, Southern Research Station.

Webb, E. K., Pearman, G. I., & Leuning, R. (1980). Correction of flux measurements for density effects due to heat and water-vapor transfer. *Quarterly Journal of the Royal Meteorological Society*, *106*(447), 85–100. https://doi.org/10.1002/qj.49710644707

Wever, L. A., Flanagan, L. B., & Carlson, P. J. (2002). Seasonal and interannual variation in evapotranspiration, energy balance and surface conductance in a northern temperate grassland. *Agricultural and Forest Meteorology*, *112*(1), 31–49. https://doi.org/10.1016/S0168-1923(02)00041-2

Wickham, J. D., Wade, T. G., & Riitters, K. H. (2013). Empirical analysis of the influence of forest extent on annual and seasonal surface temperatures for the continental United States. *Global Ecology and Biogeography*, *22*(5), 620–629. https://doi.org/10.1111/geb.12013

Wilson, K. B., & Baldocchi, D. D. (2000). Seasonal and interannual variability of energy fluxes over a broadleaved temperate deciduous forest in North America. *Agricultural and Forest Meteorology*, *100*(1), 1–18. https://doi.org/10.1016/S0168-1923(99)00088-X

Winckler, J., Reick, C. H., Luyssaert, S., Cescatti, A., Stoy, P. C., Lejeune, Q., … Pongratz, J. (2019). Different response of surface temperature and air temperature to deforestation in climate models. *Earth System Dynamics*, *10*(3), 473–484. https://doi.org/10.5194/esd-10-473-2019

Woodwell, G. M., Hobbie, J. E., Houghton, R. A., Melillo, J. M., Moore, B., Peterson, B. J., & Shaver, G. R. (1983). Global deforestation – Contribution to atmospheric carbon-dioxide. *Science*, *222*(4628), 1081–1086. https://doi.org/10.1126/science.222.4628.1081

Wutzler, T., Lucas-Moffat, A., Migliavacca, M., Knauer, J., Sickel, K., Šigut, L., … Reichstein, M. (2018). Basic and extensible post-processing of eddy covariance flux data with REddyProc. *Biogeosciences*, *15*(16), 5015–5030. https://doi.org/10.5194/bg-15-5015-2018

Zhai, J., Liu, R. G., Liu, J. Y., Zhao, G. S., & Huang, L. (2014). Radiative forcing over China due to albedo change caused by land cover change during 1990–2010. *Journal of Geographical Sciences*, *24*, 789–801. https://doi.org/10.1007/s11442-014-1120-4

Zhang, Q., Ficklin, D. L., Manzoni, S., Wang, L. X., Way, D., Phillips, R. P., & Novick, K. A. (2019). Response of ecosystem intrinsic water use efficiency and gross primary productivity to rising vapor

pressure deficit. *Environmental Research Letters*, *14*(7). https://doi.org/10.1088/1748-9326/ab2603

Zhang, Q., Manzoni, S., Katul, G., Porporato, A., & Yang, D. W. (2014). The hysteretic evapotranspiration – Vapor pressure deficit relation. *Journal of Geophysical Research-Biogeosciences*, *119*(2), 125–140. https://doi.org/10.1002/2013jg002484

Zhou, S., Williams, A. P., Berg, A. M., Cook, B. I., Zhang, Y., Hagemann, S., … Gentine, P. (2019). Land–atmosphere feedbacks exacerbate concurrent soil drought and atmospheric aridity. *Proceedings of the National Academy of Sciences of the United States of America*, *116*(38), 18848–18853. https://doi.org/10.1073/pnas.1904955116

SUPPORTING INFORMATION

Additional supporting information may be found online in the Supporting Information section.

How to cite this article: Zhang Q, Barnes M, Benson M, et al. Reforestation and surface cooling in temperate zones: Mechanisms and implications. *Glob Change Biol*. 2020;26:3384–3401. https://doi.org/10.1111/gcb.15069